

MASTER

NAA-SR-2399

COPY

ORGANIC MODERATED REACTOR EXPERIMENT
QUARTERLY PROGRESS REPORT
APRIL - JUNE 1957

AEC Research and Development Report



ATOMICS INTERNATIONAL

A DIVISION OF NORTH AMERICAN AVIATION, INC.

DISCLAIMER

This report was prepared as an account of work sponsored by an agency of the United States Government. Neither the United States Government nor any agency thereof, nor any of their employees, makes any warranty, express or implied, or assumes any legal liability or responsibility for the accuracy, completeness, or usefulness of any information, apparatus, product, or process disclosed, or represents that its use would not infringe privately owned rights. Reference herein to any specific commercial product, process, or service by trade name, trademark, manufacturer, or otherwise does not necessarily constitute or imply its endorsement, recommendation, or favoring by the United States Government or any agency thereof. The views and opinions of authors expressed herein do not necessarily state or reflect those of the United States Government or any agency thereof.

DISCLAIMER

Portions of this document may be illegible in electronic image products. Images are produced from the best available original document.

NAA-SR-2399
REACTORS-POWER
48 PAGES

ORGANIC MODERATED REACTOR EXPERIMENT
QUARTERLY PROGRESS REPORT
APRIL - JUNE 1957

EDITED BY
C. A. TRILLING

ATOMICS INTERNATIONAL

A DIVISION OF NORTH AMERICAN AVIATION, INC.
P.O. BOX 309 CANOGA PARK, CALIFORNIA

CONTRACT: AT(11-1)-GEN-8
ISSUED: DECEMBER 31, 1958



DISTRIBUTION

This report has been distributed according to the category "Reactors-Power" as given in "Standard Distribution Lists for Unclassified Scientific and Technical Reports" TID-4500 (14th Ed.), October 1, 1958. A total of 625 copies was printed.



PREFACE

This report comprises a comprehensive review of technical progress on the Organic Moderated Reactor Experiment (OMRE), which is located at the National Reactor Testing Station at Arco, Idaho. This is the fifth report of the series, and covers the period from April 1, 1957 through June 30, 1957.

Previous reports in the series are as follows:

NAA-SR-1700 OMRE First Progress Report October, 1955 - July, 1956
NAA-SR-1800 OMRE Quarterly Progress Report August - October, 1956
NAA-SR-1850 OMRE Quarterly Progress Report November - December, 1956
NAA-SR-2150 OMRE Quarterly Progress Report January - March, 1956

This report is based upon studies conducted for the Atomic Energy Commission under Contract AT(04-3)-88.



TABLE OF CONTENTS

	Page No.
I. Reactor	7
A. Fuel Elements	7
1. Fuel Element Development and Manufacture	7
2. Attachment of Thermocouples to Fuel Elements	7
3. Surface Temperature Measurement of Fuel Plates	8
B. Control Rod Test and Development	11
II. Instrumentation	14
III. Auxiliary Systems and Equipment	15
A. Electrical Equipment	15
B. Fuel Handling Equipment	15
C. Shielding Studies on Fuel Handling Equipment	16
IV. Research Program	20
A. Process Development	20
1. Second Organic In-Pile Loop Experiment	21
2. Heat Transfer and Fouling Studies	21
3. Purification Studies	25
B. Corrosion Studies	26
C. Physical Properties of Organic Coolants	26
1. Carbon and Hydrogen Analyses of Irradiated Coolants	26
2. Density of Irradiated Coolants	28
3. Viscosity of Irradiated Ortho-, Meta-Terphenyl	34
4. Melting Point of Irradiated Diphenyl	34
5. Distillation Curves of Irradiated Coolants	40
6. Ortho-, Meta-Terphenyl OMRE Acceptance Tests	40

LIST OF TABLES

I. Heat Transfer Data and Results for Santowax O-M	21
II. Santowax O-M Fouling Runs - - Summary of Average Conditions . .	25
III. OMRE Acceptance Test Determinations	42



LIST OF FIGURES

	Page No.
1. OMRE Fuel Handling Coffin with Supplemental Shields	17
2. OMRE Fuel Handling Coffin Extension	19
3. Variation of the Heat Transfer Coefficient for Santowax O-M with Bulk and Surface Temperature	23
4. Variation of Heat Transfer Coefficient During Santowax O-M Fouling Studies	24
5. Purification Loop Flow Diagram	27
6. Carbon-to-Hydrogen Ratio of Irradiated Organic Coolants	29
7. Hydrogen Density of Irradiated Diphenyl	30
8. Hydrogen Density of Irradiated Isopropyl Diphenyl	31
9. Hydrogen Density of Irradiated Ortho-, Meta-Terphenyl	32
10. Hydrogen Density of Irradiated Santowax R	33
11. Density of Irradiated Ortho-, Meta-Terphenyl	35
12. Density of Irradiated Santowax R	36
13. Density of Irradiated Diphenyl	37
14. Viscosity of Irradiated Ortho-, Meta-Terphenyl	38
15. Melting Point of Irradiated Diphenyl	39
16. Distillation Temperature Curve for Irradiated Diphenyl	44
17. Distillation Temperature Curve for Irradiated Isopropyl Diphenyl	45
18. Distillation Temperature Curve for Irradiated Santowax R	46
19. Distillation Temperature Curve for Irradiated Ortho-, Meta-Terphenyl	47
20. Distillation Temperature Curve for Irradiated Diphenyl (Alternate Feed and Bleed Cycles)	48



I. REACTOR

A. FUEL ELEMENTS

1. Fuel Element Development and Manufacture (M. H. Binstock)

The fuel element being fabricated for the OMRE is composed of thin flat plates assembled into a rectangular stainless-steel box. The fuel plates are made of stainless steel-uranium oxide cores clad in stainless steel. The mechanically-assembled rectangular fuel box is welded to end adapters to complete the fuel element fabrication.

During this quarter, the required thirty-six elements were essentially completed. Several necessary changes were made: These included machining the head extension, adding a spring to the locking mechanism, and several minor changes in thermocouple attachments.

During the fabrication, one assembled fuel box was completely disassembled and the fuel plates were found to be easily recoverable. This proves that the mechanical "tabbed" assembly method reduces the amount of scrap plates. During the week of June 26, 1957, twenty-eight elements were transferred to the OMRE site and the field work necessary to complete the thermocoupled fuel elements was started. The remaining eight elements are presently in storage awaiting shipment.

The total scrap and reject rate for the entire process was 15 percent, which was well below our original estimate of 20 percent. Our unaccounted-for material was less than 30 grams, which is well below expectations as described in the feasibility report.

Process specifications were written and will be issued internally. A topical report has been written and should be issued during the next quarter.

The thermocouple attachments were completed with a minimum of trouble. The calibration of the thermocouple assembly was started (see Section I, A, 3).

2. Attachment of Thermocouples to Fuel Elements (S. Bain)

OMRE exit coolant and fuel plate surface temperatures will be measured by means of thermocouple assemblies installed in seven OMRE fuel elements. Installation of the thermocouple assemblies has been completed and the fuel elements have been shipped to the reactor site.



Each of the seven fuel elements contains five thermocouple assemblies; four are positioned on a fuel plate and one is located in the top assembly pin. Of the four located on the fuel plate, three monitor the fuel plate surface temperature; the fourth thermocouple assembly monitors the temperature of the exit coolant "hot stream." The fifth thermocouple assembly monitors the temperature of the exit coolant "cold stream." Variation in neutron flux within a fuel element accounts for the fact that the coolant flowing along the edges of the element is hotter than coolant flowing in the center.

All of the thermocouple assemblies are fabricated from 1/16-inch Type 304 swaged stainless-steel sheath containing chromel and alumel wires 0.005 inch in diameter and insulated with MgO. The thermocouple assemblies used to measure the exit coolant temperatures are Heliarc welded at one end to serve the dual purpose of forming and sealing the thermocouple junction.

3. Surface Temperature Measurement of Fuel Plate (S. Sudar, S. Bain)

An investigation has been conducted to determine the magnitude of error in surface temperature measurements of the OMRE fuel plate, utilizing a chromel-alumel thermocouple assembly. The extent of error inherent in the thermocouple assembly indicates the need for a calibration of the thermocouple assembly under simulated reactor fluid velocity and heat flux conditions. Apparatus for the purpose of this calibration has been fabricated and tested and a revised design is presently being constructed.

The OMRE fuel plate surface thermocouple assembly consists of chromel-alumel wires, 0.005 inch in diameter, extending approximately 0.25 inch from a 1/16-inch-diameter stainless-steel sheath and spot welded to the fuel plate surface. The bared lead wires between the thermocouple junctions and the swaged steel sheath containing MgO are enclosed in finely-drawn quartz tubes approximately 0.006 inch ID and 0.013 inch OD. The wires are each welded separately to the steel surface, and the resulting chromel-steel, alumel-steel junctions are approximately 0.013 inch apart. Spanning the two quartz tubes are two stainless-steel straps (0.015 inch wide, 0.060 inch long, and 0.003 inch thick) which are welded to the plate surface to restrict movement of the quartz-enclosed thermocouple lead wires.



This thermocouple assembly was selected for use in the OMRE fuel element after a series of tests indicated it could be easily and uniformly attached to the plate surface, was stable under OMRE flow conditions, and was capable of calibration. Its nuclear characteristics had been previously considered and found to be satisfactory.

The error in measurement of the fuel plate surface temperature, utilizing a thermocouple assembly in which the junction and lead wires are exposed to the coolant stream, is due in part to the cooling of the junction caused by the conduction of heat along the lead wires away from the junction. Heat is transferred from the lead wires to the coolant stream by convection. The magnitude of this error factor is dependent upon the following quantities:

- 1) Diameter of the thermocouple wires.
- 2) Coefficient of heat transfer from the lead wires to the stream.
- 3) Thermal conductivities of the heat transfer surface and the thermocouple wires.
- 4) Temperature gradient from the surface to the coolant stream.

Another factor contributing to the error in the fuel plate temperature measurement is the extremely thin thermal boundary layer characteristic of the organic coolant. At coolant stream conditions of 500°F and 15 fps, the thermal boundary layer is approximately 0.0008 inch. Theoretically, the total surface-to-coolant temperature drop occurs within this distance. The fact that this distance is even smaller at the thermocouple junction due to local increased turbulence indicates that the junction is partly exposed to a temperature intermediate between surface and bulk coolant temperatures. The error due to loss of heat from the junction due to conduction and convection is more significant because of the thin thermal boundary layer. Almost all of the quartz insulated lead wires are in the bulk coolant temperature zone.

An initial test was conducted to determine the extent of the error inherent in the "quartz tube" thermocouple assembly. The test section consisted of a stainless-steel plate (1 inch wide x 18 inches long x 0.030 inch thick) which formed a common wall between a rectangular duct (1 inch wide x 18 inches long x 0.135 inch thick) and a molten lead bath extending along the entire length of the duct. Organic coolant was circulated through the duct. Two groups of thermocouples were



attached to the steel plate surface. Each group of thermocouples consisted of a "quartz tube" assembly and a "copper disc" assembly on the organic side of the steel plate, and a reference thermocouple on the lead side. This test section afforded geometric similarity to the OMRE fuel element.

Results of the test utilizing the lead bath heat source indicated that the "copper disc" thermocouple assembly gave a slightly more accurate surface temperature measurement. However, its disadvantages — difficulty of brazing to the fuel plate and increased disturbance to the reactor neutron flux — were not offset by the slight gain in accuracy. At the conclusion of this test, it was decided to install the "quartz tube" thermocouple assembly in the OMRE fuel elements.

Discrepancies in the temperature measurements as indicated by the two groups of thermocouple assemblies employed in the "molten lead bath" test section indicated that an accurate thermocouple calibration required changes in design of the test apparatus.

A test section was designed to obtain data for calculation of the surface temperature of the test plate. Reactor fuel plate heat generation and cooling conditions are simulated by electrically heating a stainless-steel plate which is contained in the center of a rectangular duct through which the organic coolant is circulated. Four samples of the "quartz tube" thermocouple assemblies will be attached to the electrically-heated test plate to determine the extent of variation in temperature measurements attributable to variation in thermocouple assemblies.

True temperature of the test plate will be calculated by utilizing the relationship:

$$q = hA (t_s - t_c),$$

where

q = heat input,

h = heat transfer coefficient from the plate to the coolant,

A = heat transfer area,

t_s = plate surface temperature,

t_c = coolant temperature.



The test apparatus is designed to operate at 60 psig, a maximum coolant velocity of approximately 20 fps, a maximum heat flux of 200,000 Btu/hr-ft², and a maximum coolant temperature of 600°F. At the OMRE design velocity of 15 fps and coolant temperature of 500°F, the expected temperature gradient from plate surface to the coolant is 200°F. The average OMRE design flux is 90,000 Btu/hr-ft² and the peak flux is 300,000 Btu/hr-ft².

A test apparatus was completed, but warpage of component parts during fabrication did not permit a satisfactory pressure seal. Remachining of the warped section has been completed. A pressure test of the section at approximately double operating pressure showed it to be leak tight. Reassembly of the test apparatus is now in progress.

B. CONTROL ROD TEST AND DEVELOPMENT (H. Strahl)

Performance tests were continued after those previously reported. Three additional tests (Nos. 4, 5, and 6) were completed during this period. As a result of these tests, the reactor units were modified and installed in the OMRE.

The "start-up accident" study which was employed in establishing the parameters of the safety system showed that the time interval from a scram signal until the poison elements begin their downward motion should be 0.050 second or less. During test No. 4, excessive time delays were measured in the ball release mechanism. The test was concluded after eight intentional scrams, when the response measurements revealed an average of 0.070 second was required for the balls to release and the rods to start moving.

The results of a preliminary stress analysis performed on the ball release mechanism indicated that the balls were excessively loaded. Prior to test No. 5, the rack was remachined to utilize four balls instead of the original two.

Test No. 5 was concluded after 1090 cycles when excessive time delays were again measured in the ball release mechanism. During the test, the diphenyl temperature was increased to 730°F and then lowered to 300°F. The rod was cycled 275 times while the temperature was being increased to 700°F. The rod was then cycled 525 times while the diphenyl temperature was between 700 and 730°F. The remaining 290 cycles were completed while the diphenyl was cooling down to 300°F.



The diphenyl temperature was being decreased when the excessive time delays were measured. Disassembly revealed that the solenoid spring housing had unscrewed 1/8 inch. This increased the ball release stroke from 3/8 inch to 1/2 inch and also decreased the compression on the release spring.

The rod "seated" Microswitch failed to function after cycle No. 40 of test No. 5. Disassembly at the conclusion of the test revealed that the roller was damaged from being struck with the actuator mounted on the hanger rod. This switch was positioned to be as far as possible from the hanger rod and still make contact. It could not be positioned on the snubber, as is the case in the reactor, due to the small tank size at the snubber in the test assembly. Therefore, the switch was mounted 20 inches above the snubber where the magnitude of the rod whip was greater than it would be if the switch was mounted on the snubber.

During this test, data was obtained on the position of the control rod after release as a function of time. This data was obtained by utilizing the signal from a magnetic pickup, recorded on a Consolidated Electrodynamics Corporation Type 5-116 oscilloscope.

Prior to test No. 6, all screw joints were pinned to prevent possible unscrewing. An external 3- to -1 gear reduction was installed between the regulating drive motor and the gear box. This additional reduction was necessary because the regulating motor would not drive the rod up except at the maximum setting of the Variac controller. The specifications require that the regulating rod speed be continuously variable from a small value to its maximum velocity because of the uncertainties involved in the many parameters of the reactor. The Metron speed changers originally utilized in the regulating and shim control boxes were replaced with Boston gears.

No further difficulties were encountered with the ball release mechanism during test No. 6. The elapsed time from the moment a scram was initiated until the rods started to move was consistently between 0.025 and 0.030 second throughout the test.

The 3- to -1 external gear reduction allowed the regulating drive motor to operate at higher speeds where sufficient torque was available to drive the rods at the required speeds. The regulating drive was cycled 1000 times through its 5.1 inch stroke for a functional check of the controlling components and the 3- to -1 speed reducer.



Conformance tests were also completed on the shim rod drive. The drive unit was within the specified limits for velocity, drift, and fine manual control.

At the conclusion of test No. 6, the test unit was disassembled and all parts carefully inspected. All the components appeared acceptable for reactor installation except the rod "seated" switch which had been damaged as previously described.

Following test No. 6, the OMRE reactor control-safety rods were modified and installed. Time response measurements recorded during a series of scrams were nearly identical to those recorded during the tests.



II. INSTRUMENTATION (E. Matlin)

The outlet gas flow meter was changed to a local indicating meter. The original design called for a remote indication. However, it was impossible to obtain a supplier of a remote indicating flow meter to our required accuracy of below 0.7 scfm.

The pressure regulator controlling the nitrogen pressure to the control rod seals was replaced with a differential-pressure-actuated control valve in order to maintain a constant differential pressure between the seals and the core tank. This eliminated the necessity of manual readjustment of the control-rod pressure setting to accommodate changes in reactor tank pressure.

Spring-loaded back-pressure regulators on the purge gas outlet have been replaced with pilot-operated motor-controlled valves in order to improve the control of the reactor pressure.

The diaphragm-protected silicone-oil-filled compound gauges were replaced with systems employing electrical transducers mounted directly on the diaphragm protectors. This was done because of unsatisfactory operation of the compound gauges.



III. AUXILIARY SYSTEMS AND EQUIPMENT

A. ELECTRICAL EQUIPMENT (R. B. Hall)

All facilities vent motors were interlocked with the CO₂ fire extinguishing system. The interlocking between the motor starters and the fire control panel prevents the vent fans from ejecting CO₂ out of the building vents.

A complete functional test was conducted on the induction heating installation at the OMRE site. Large-sized piping and vessels were successfully heated and controlled. Temperature rate-of-rise problems found to be existing dealt with small-sized pipe in short lengths in the purification system and in valves throughout the system. Resistor banks were installed to permit voltage reduction on the induction heating circuits with a fast temperature rate of rise. Electrical cartridge heaters were installed on valves to correct low temperatures and slow rates of rise; thus, valves are now heated with induction coils and resistance cartridge heaters.

B. FUEL HANDLING EQUIPMENT (H. Jarvis)

For the purpose of handling fuel at the reactor and shipping it to a hot cell at a remote point, several units have been designed from which assemblies can be made adaptable to the various tasks to be accomplished. These units are listed below:

- 1) The cask proper with the fuel pick-up tool.
- 2) An auxiliary shield for use in the reactor; this is required to protect operating personnel against streaming while the fuel is passing from the organic liquid to the cask.
- 3) A removable support frame for the cask when it is used at the reactor for handling fuel.
- 4) A frame for mounting the cask horizontally on a truck for highway shipment of fuel; provision is made also to facilitate the rotation of the cask from horizontal to vertical or vice versa, whichever is necessary when loading or unloading the cask from the truck.



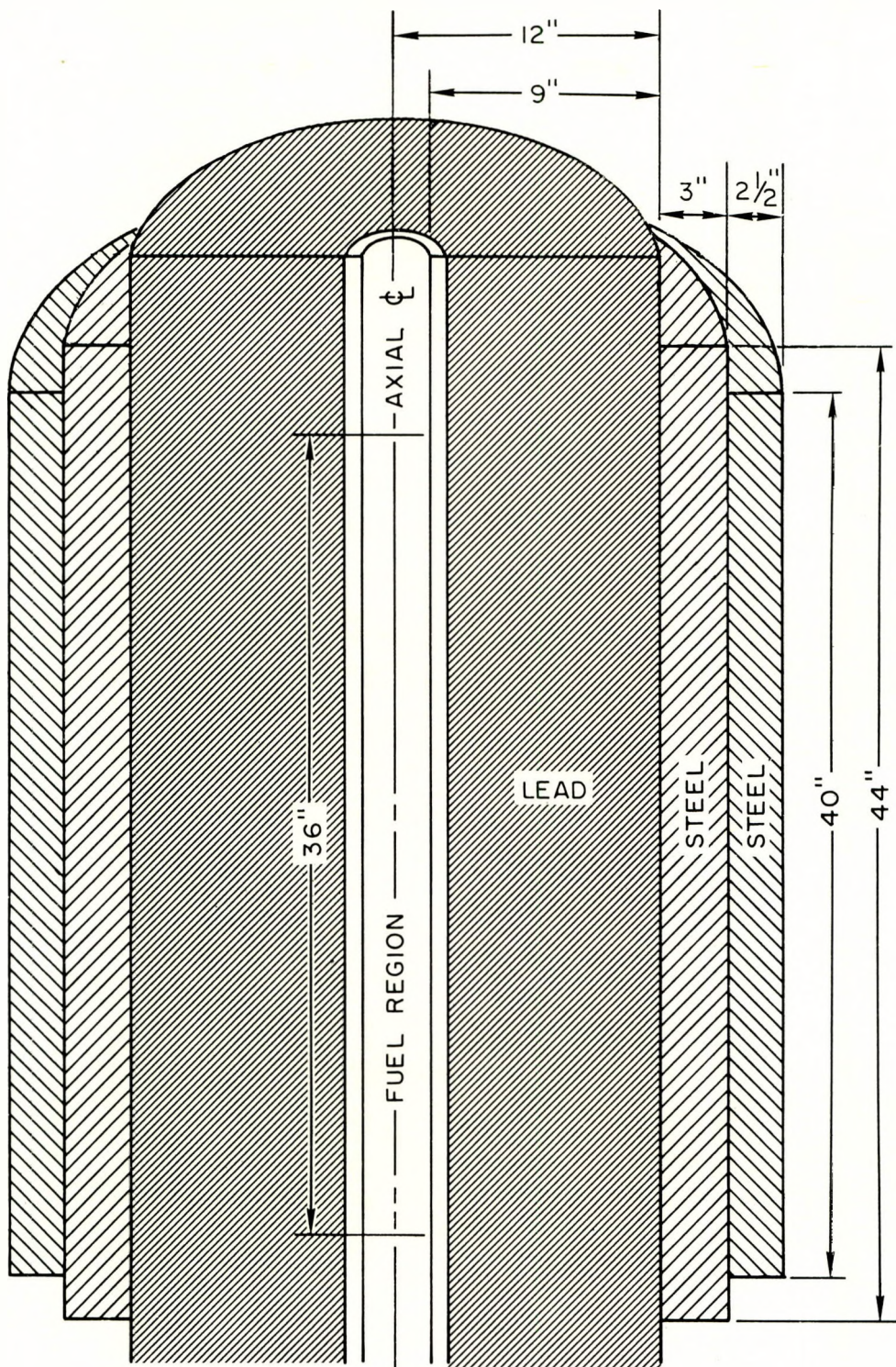
- 5) Several supplemental shields have been designed. One or more of these may be attached to the cask to provide additional shielding when the radioactivity of the fuel shipped is above average.
- 6) A cooling pump and heat-exchanger assembly to dissipate afterglow heat of the fuel to avoid fuel temperatures in excess of those encountered during operation of the reactor.

C. SHIELDING STUDIES ON FUEL HANDLING EQUIPMENT (D. S. Duncan)

1. Fuel Handling Coffin

Results of a previous analysis have indicated that 10.5 inches of lead would be required for shielding the OMRE fuel handling coffin. However, due to the experimental nature of this reactor and the high cost of transportation of a coffin with 10.5-inch lead walls, it is more economical to design a coffin with a thin fixed shield (perhaps 8 or 9 inches of lead) and, when the activity of the spent fuel element requires it, to supplement this with sufficient steel to meet ICC shipping requirements. Using this philosophy, the shipping coffin was designed to consist of three parts: the basic coffin and two supplemental steel shields. The inner supplemental shield will be used when shipping an "average" OMRE element ("average" corresponds to an element which has been operated in the reactor for 115 days at a power level of 0.64 Mw and allowed to cool in the storage rack for 30 days). The outer supplemental shield will be used in conjunction with the inner shield when shipping the "hottest" expected element (an element referred to as the "hottest" expected element is defined as one which has been operated in the reactor for 180 days at a power level of 1.00 Mw and allowed to cool for 24 hours). Figure 1 is a section through the fuel handling coffin showing the required position and dimensions of the two supplemental shields and the corresponding lead thickness for the coffin. This shield configuration was designed to meet ICC shipping regulations during fuel shipment and to prevent excessive radiation from occurring at the surface of the coffin during fuel removal operations when supplemental shielding is not present.

The top shield plug for the coffin will be composed of steel, while the bottom shield plug will be composed of lead encased in 3/4 inch of steel. The required thicknesses of these two plugs for shipment of the hottest expected element are 15.25 inches of steel and 10.95 inches of lead, respectively.



LEAD DENSITY = 11.3 gm/cc
 STEEL DENSITY = 7.75 gm/cc
 1/8" - SCALE

Fig. 1. OMRE Fuel Handling Coffin with Supplemental Shields



For purposes of determining the cooling requirements for the spent fuel elements, the total heat generation rate (beta plus gamma) in the coffin due to fission product decay radiation produced by the hottest expected element was found to be 5.4×10^3 watts.

2. Fuel Handling Coffin Extension

Figure 2 shows the proposed shield configuration for the fuel handling coffin extension. This design, in conjunction with the work platform, will prevent radiation levels from exceeding 200 mr/hr at the operator position at the base of the fuel handling coffin during removal of an average OMRE element. It will also prevent radiation levels from exceeding a maximum of 10 r/hr at any location in the vicinity of the reactor vessel during the removal operation for this same element.

3. Work Platform to be Used During Fuel Removal Operation

It has been shown by a previous analysis that 4 inches of steel are required to reduce the radiation level above the work platform to 1.0 r/hr during the removal of a fuel element which had been operated at a power level of 0.64 Mw for 1000 hours and then allowed to cool for 10 hours. This element has an after-shutdown power from hard-gamma-ray-emitting fission products of approximately five times that of the average OMRE element defined above. Thus, 4 inches of steel will also be required to reduce radiation levels above the work platform to 200 mr/hr during the removal of an average OMRE element.

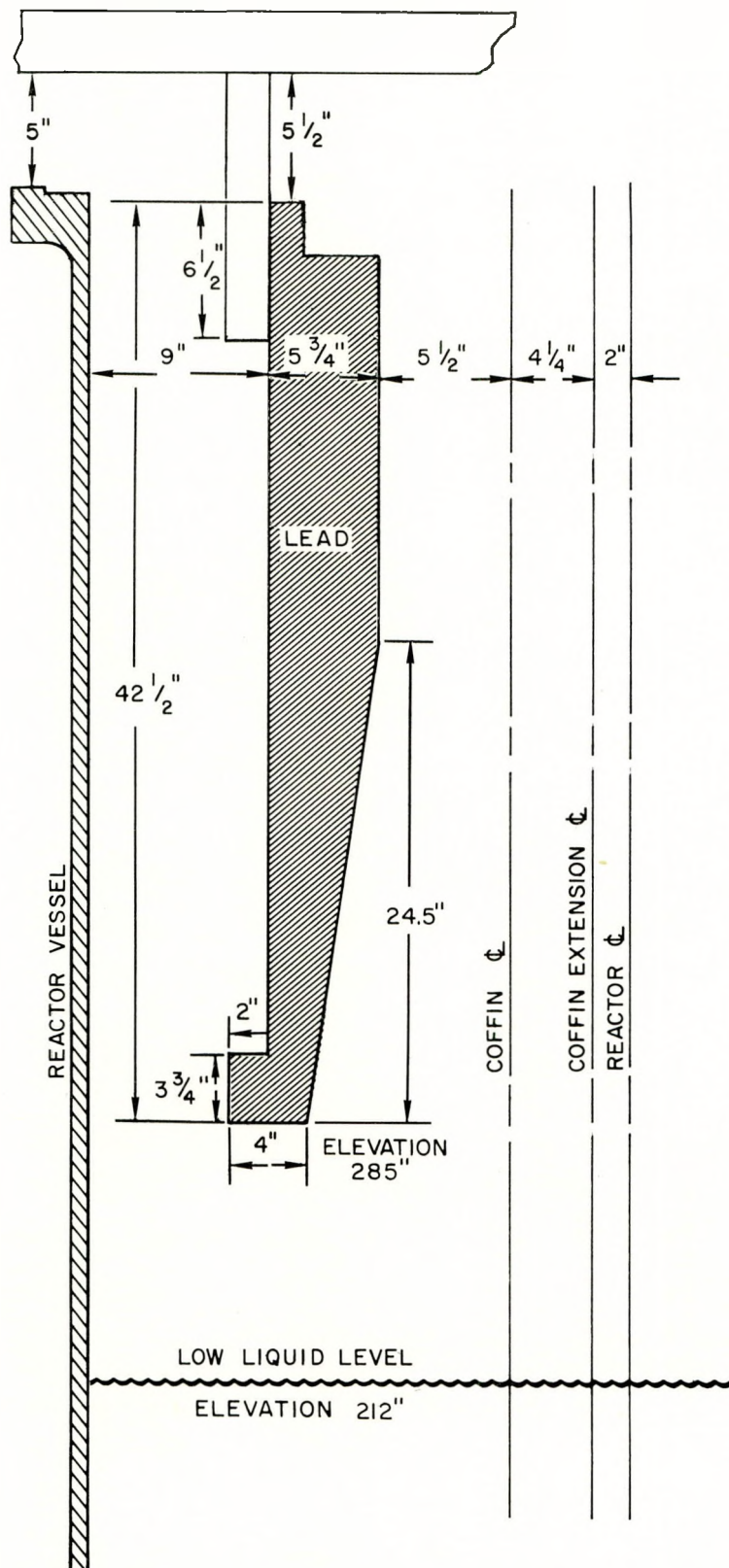


Fig. 2. OMRE Fuel Handling Coffin Extension



IV. RESEARCH PROGRAM

A. PROCESS DEVELOPMENT (D. W. Bareis)

1. Second Organic In-Pile Loop Experiment (W. N. Bley, G. C. Cox, and S. Loeb)

Work accomplished during the quarter included the hot-cell examination of the in-pile uranium heaters, the hot-cell examination of the corrosion specimens, the analysis of the neutron flux monitor wires, the determination of the physical properties of the irradiated samples, and the writing of preliminary drafts of the final report.

a. Hot Cell Examinations

The in-pile sections were cut apart so that the uranium heaters and the corrosion specimens could be observed in the MTR hot cell. The in-pile loop surfaces exposed to the organic fluid had a thin film of material which was insoluble in methyl-chloroform. In some cases, the material on the uranium heater appeared darker or less transparent than the materials on the other surfaces.

The results obtained from the corrosion specimens indicated that steel and aluminum are not affected by the organic fluids in the radiation field. Magnesium and zirconium corrosion specimens had excessive weight gains. The corrosion study results will be reported elsewhere.*

b. Neutron Flux Monitors

The analysis of the fast-and thermal-neutron flux monitor wires is being done by the MTR staff. The results should be available at the beginning of the next quarter. Until the flux data are available, the heat transfer and decomposition rate calculations cannot be completed.

c. Physical Property Determinations

Measurements of the carbon-hydrogen ratio, density, viscosity, melting point, radiolytic gas composition, and the distillation curves for the irradiated coolant samples are reported in Section IV, C of this report. Since

* W. N. Bley, N. J. Gioseffi, H. Kline, "Dynamic Corrosion Tests of Materials in Irradiated Organics," NAA-SR-2046 (to be published)



the heat capacity and thermal conductivity measurements will be delayed, the final in-pile loop report will not have the benefit of this information. A supplementary report discussing the physical property measurements for the irradiated coolant samples will be issued at a later date.

2. Heat Transfer and Fouling Studies (D. A. Huber and M. Silberberg)

Experimental forced convection heat transfer and fouling runs with unirradiated Santowax O-M (2 parts ortho-, 1 part meta-terphenyl) have been completed.

a. Heat Transfer Study

The experimental forced convection heat transfer results are listed in Table I.

TABLE I
HEAT TRANSFER DATA AND RESULTS FOR SANTOWAX O-M

Velocity (ft/sec)	Bulk Temp., (°F)	Surface Temp. (°F)	Δt (°F)	Heat Flux (Btu/hr-ft ²)	Heat Transfer Coefficient, <i>h</i> _{exp} (Btu/hr-ft ² -°F)
25.7	512	542.5	30.5	58,300	1900
24.4	537	595.5	58.5	100,000	1710
20.3	490	527.5	37.5	54,200	1430
19.7	539	595.5	56.5	74,600	1320
15.4	529	591.0	62.0	68,000	1100
5.1	482	584.0	102.0	43,300	425
25	583	691.5	108.5	193,500	1780
19.4	584	695.0	11.0	166,700	1500
14.8	589	696.5	107.5	127,300	1180
9.3	584	704.0	120.0	94,800	790
5.0	594	694.0	100.0	44,800	450
25.6	666	776.5	110.5	195,000	1770
14.8	687	785.0	98.0	115,900	1180
5.6	657	792.0	135.0	70,800	535
25.5	763	859.5	96.5	195,000	2000
14.3	752	854.5	102.5	126,000	1210
5.4	750	877.0	127.0	70,000	550
19.9	683	837	154.0	254,000	1650
9.1	691	870.0	179.0	157,200	895
5.1	685	851.0	166.0	86,400	518



In the preceding table, the data were taken over the following operating ranges:

Bulk Temperature	490 to 765°F
Surface Temperature	525 to 880°F
Film Temperature Difference	30 to 180°F
Fluid Velocity	5, 10, 15, 20, and 25 ft/sec
Nitrogen Pressure	300 psig
Heat Flux	43,000 - 254,000 Btu/hr-ft ²

Figure 3 shows the effect of temperature upon the heat transfer coefficient. No attempt was made to correlate the data with standard correlations due to the lack of information on physical property data.

b. Fouling Study

The purpose of this study was to investigate the high-temperature fouling tendencies of Santowax O-M at a heat transfer surface. A procedure identical with that used in the Santowax R fouling study was used to detect any evidence of fouling.*

Since the results for Santowax O-M were expected to agree with those for Santowax R, the following conditions were used for the initial run:

Bulk Temperature	750°F
Surface Temperature	1000°F
Fluid Velocity	15 ft/sec
Duration	48 hours

In order to observe the effect of low velocity, and to approach possible fouling conditions gradually, the heater surface temperature was then lowered to 900°F, and tests were carried out at a fluid velocity of 10 ft/sec for 26 hours, and at a fluid velocity of 5 ft/sec for 50 hours.

Table II lists the average conditions for the three runs and Fig. 4 shows the variation of average heat transfer coefficient with time. The local and average coefficients in all three runs remained constant throughout the runs, indicating that the rate of fouling of the heat transfer surface was negligible under the above conditions.

* C. A. Trilling, "OMRE Quarterly Progress Report, January - March, 1957," NAA-SR-2150, February 15, 1958, p. 32.

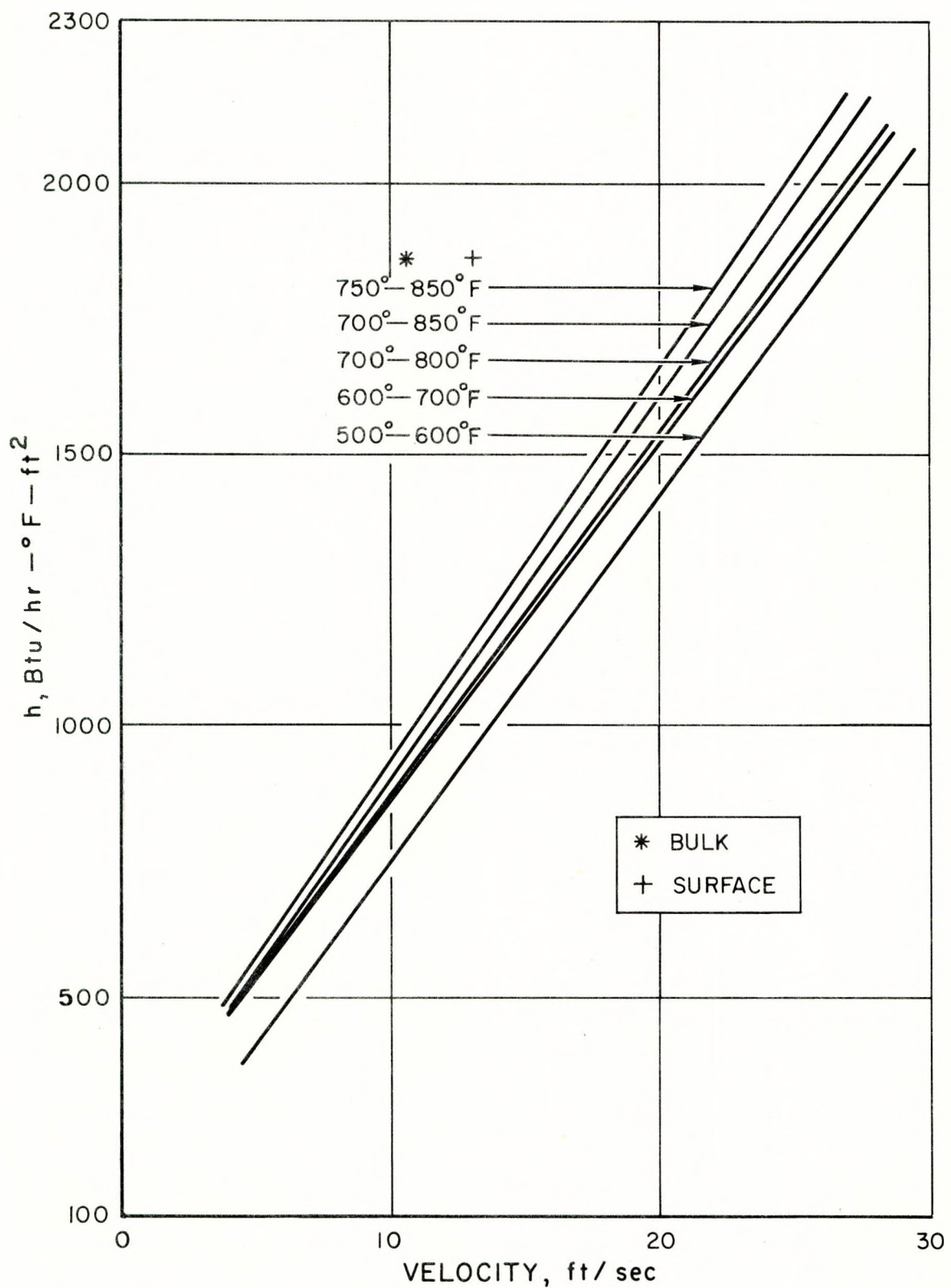


Fig. 3. Variation of the Heat Transfer Coefficient for Santowax O-M with Bulk and Surface Temperature

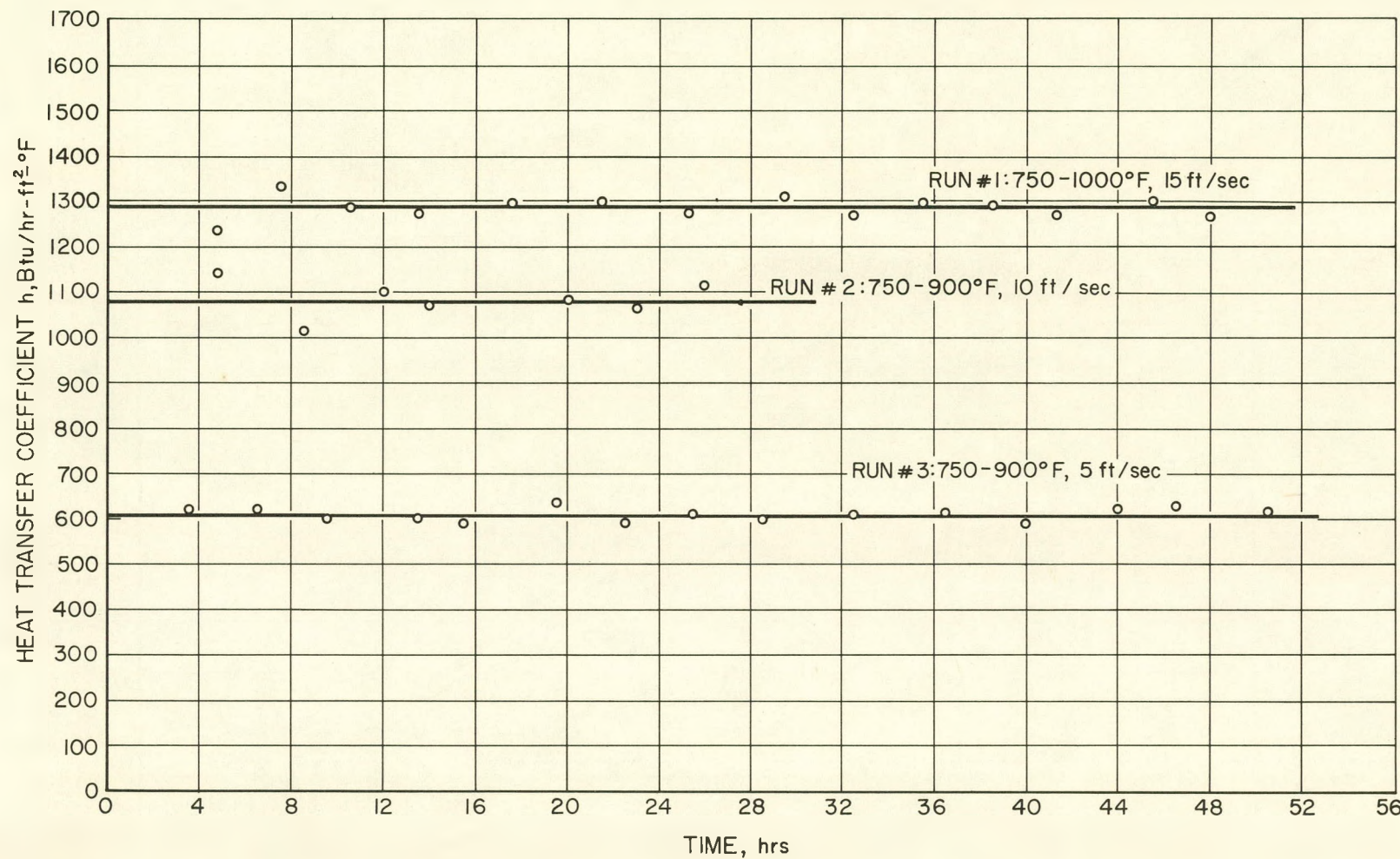


Fig. 4. Variation of Heat Transfer Coefficient During Santowax O-M Fouling Studies





TABLE II
SANTOWAX O-M FOULING RUNS
SUMMARY OF AVERAGE CONDITIONS

Run	Nominal Condition	Velocity (ft/sec)	Elapsed Time Hrs.	Avg. Max. Surface Temp. (°F)	Avg. Surface Temp. (°F)	Avg. Bulk Temp. (°F)	Avg. Temp. Diff. (°F)	Avg. Flux (Btu/hr-ft ² -°F)	Avg. Heat Transfer (Btu/hr-ft ² -°F)
1	750-1000	15	48	1008	976	756	220	284,000	1290
2	750-900	10	26	925	895	753	141	152,000	1080
3	750-900	5	50.5	924	896	745	148	90,000	609

Defouling runs have been made at increased fluid velocities and lower temperatures in an attempt to remove the deposited film. Analysis of this data will be conducted during the next quarter.

3. Purification Studies (W. E. Duffy and G. O. Haroldsen)

During the early part of May, the OMRE Purification System at the reactor site was checked out. Kerosene was used to flush out any dirt present after fabrication. The kerosene was circulated between the various tanks by means of a pump temporarily connected to the system. A filter was placed in the circuit to indicate when the kerosene was free of suspended materials. The kerosene was removed and the system heated and purged with nitrogen.

A eutectic mixture of diphenyl and ortho-terphenyl was used to check out the operation of the purification system. The low melting point (70°F) of this material made it easy to handle during start-up. The first distillation run indicated that there was residual kerosene in the system. A temporary cold trap was installed downstream of the permanent vapor trap to collect the kerosene vapors.

The results of the earlier vapor trap studies at Canoga Park were verified at the OMRE site when it was found that close temperature control of the vapor trap was required to prevent carry-over of diphenyl into the vacuum system.

A laboratory distillation loop will be built to study the distillation characteristics of the OMRE coolant. A schematic diagram of the loop is shown



in Fig. 5. Interchangeable-plate and packed-type glass columns will be used to observe these characteristics as a function of the operating conditions. The instrumentation will allow the accurate measurement of material and heat balances on the loop components.

Fabrication of the feed, product, and waste tanks is complete. The various components will be assembled on receipt of the glass columns from the vendor.

B. CORROSION STUDIES (H. E. Kline)

Examination of all corrosion specimens from the in-pile and out-of-pile sections of the NAA-20 loops was completed during this quarter and a final topical report was written. This report will be issued as NAA-SR-2046.* The information obtained showed that aluminum, Types 304 and 410 stainless steel, carbon steel, and 4130 alloy steel exhibited good to excellent corrosion resistance to irradiated polyphenyls. Magnesium and zirconium were unsatisfactory due respectively to oxidation and hydriding. Integrated neutron fluxes of the order of 2×10^{19} nvt thermal and 10^{18} nvt fast did not affect the corrosion resistance of the materials studied.

This project was completed and terminated on June 30, 1957.

C. PHYSICAL PROPERTIES OF ORGANIC COOLANTS (R. H. J. Gercke, G. Asanovich, and R. A. Baxter)

1. Carbon and Hydrogen Analyses of Irradiated Coolants

The carbon and hydrogen content of irradiated coolants was determined in order to measure the effect of coolant decomposition on moderating ability. These analyses were carried out on samples of irradiated coolants studied in the Second Organic In-Pile Loop Experiment, viz. diphenyl, isopropyl diphenyl, ortho- meta-terphenyl, and Santowax R. The radiation-decomposed samples were obtained during operation of this experiment at the Materials Testing Reactor. Details of this experiment are given in Section IV, A, 1 of this report. The starting mixture of ortho-, meta-terphenyl used in the loop test was synthetically compounded and contained 2/3 by weight ortho-terphenyl and 1/3 by weight meta-terphenyl.

* W. N. Bley, op. cit.

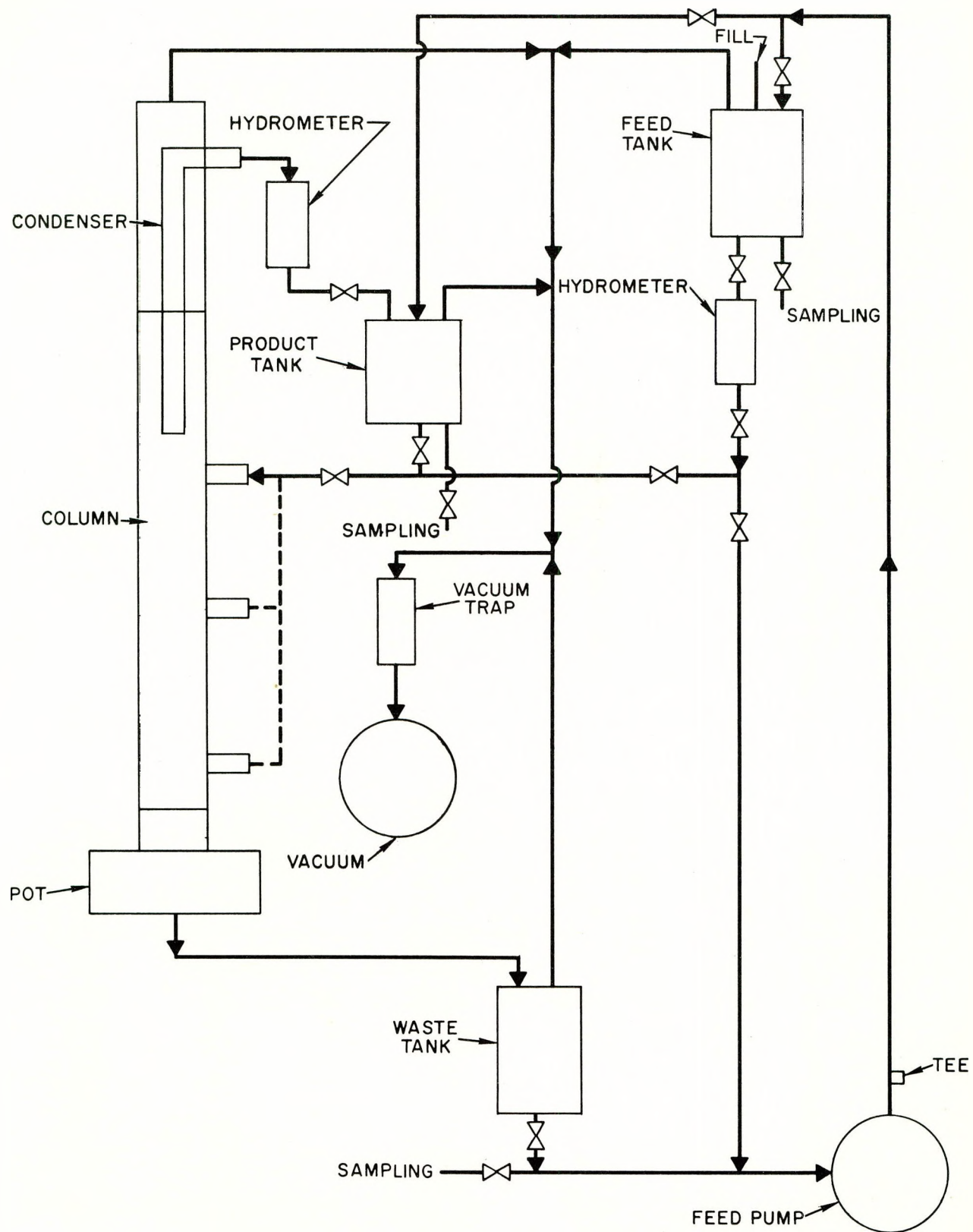


Fig. 5. Purification Loop Flow Diagram



A macroscopic combustion train was employed in determining carbon and hydrogen content. The sample size was 0.2 gm. The probable errors (absolute) were found to be ± 0.03 percent for hydrogen and ± 0.11 percent for carbon. The limits of error illustrated in Fig. 6 (carbon-to-hydrogen ratio vs high-boiler-residue content) are based upon an estimated absolute error of ± 3 percent for percent high-boiler-residue content and the experimentally determined value of ± 0.03 percent for hydrogen.

The carbon-to-hydrogen ratio increases with increasing high-boiler-residue concentration for all four coolants studied. The increase in this ratio due to a change in high-boiler residue from none to 35 percent by weight is as follows:

	$\%$
Isopropyl Diphenyl	4.8
Diphenyl	3.1
Ortho-, Meta-Terphenyl	1.8
Santowax R	1.6

Using the density data for the coolants presented in Section IV, C, 2 and the density of isopropyl diphenyl from the previous quarterly report, N_H values (hydrogen atoms per cm^3) were calculated over the range 300 to 850°F. The variation of hydrogen density (N_H) as a function of temperature with high-boiler-residue content as a parameter is illustrated for each coolant in Figs. 7, 8, 9, and 10.

It is of interest that hydrogen density (and consequently moderating ability) increases with the build-up of radiation decomposition products. This occurs because the density of the decomposition products is great enough to more than offset the loss in hydrogen due to the greater C/H ratio of the higher molecular weight decomposition products.

Preliminary results indicate that changes in coolant density because of changes in gas solubility are negligible.

2. Density of Irradiated Coolants

The effects of radiation on the density of ortho-, meta-terphenyl and Santowax R were determined over the temperature range 300 to 850°F, while the density of irradiated diphenyl was determined from 300°F to its normal boiling point. Radiation-decomposed samples used in these determinations were obtained

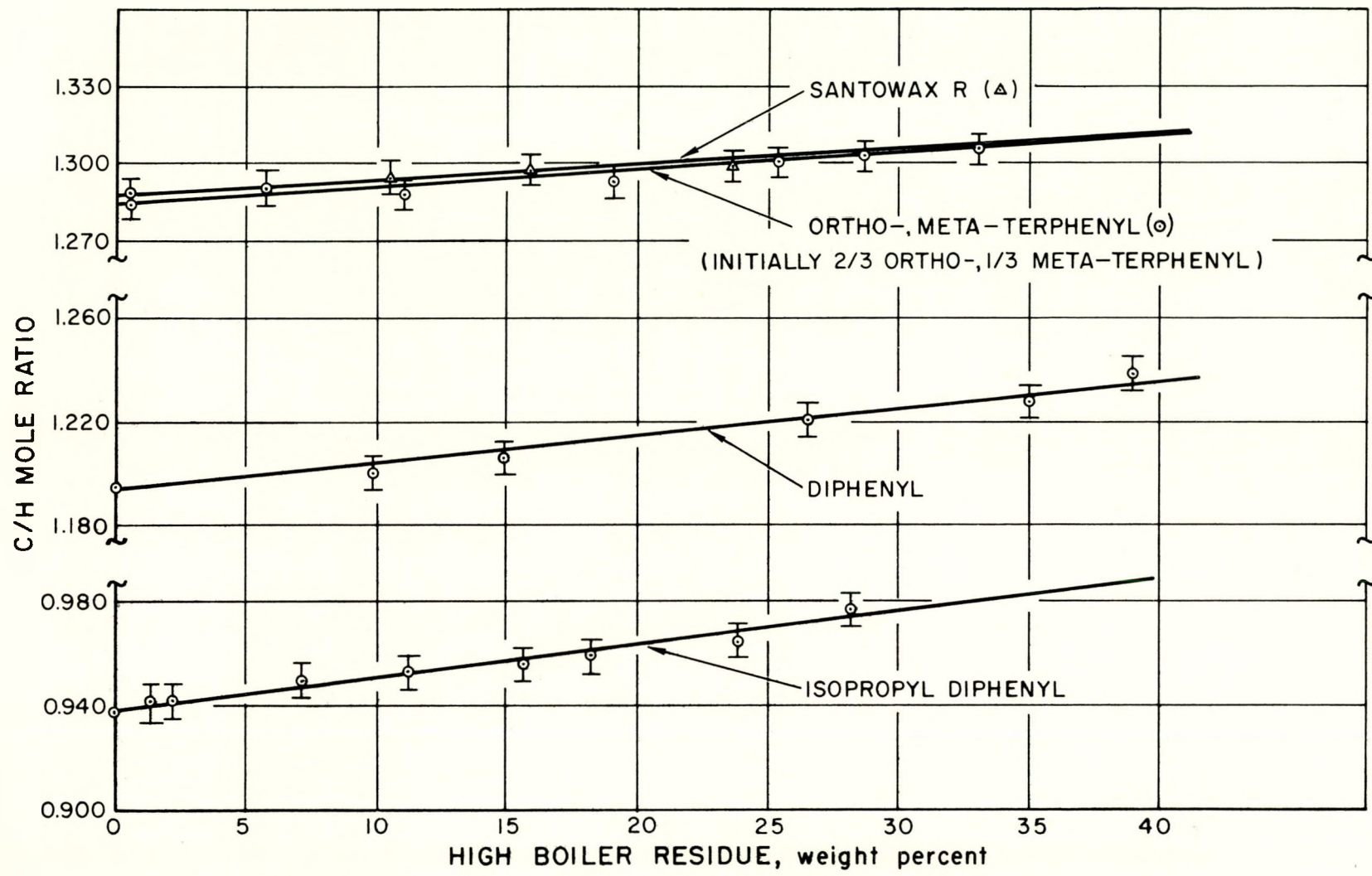


Fig. 6. Carbon-to-Hydrogen Ratio of Irradiated Organic Coolants

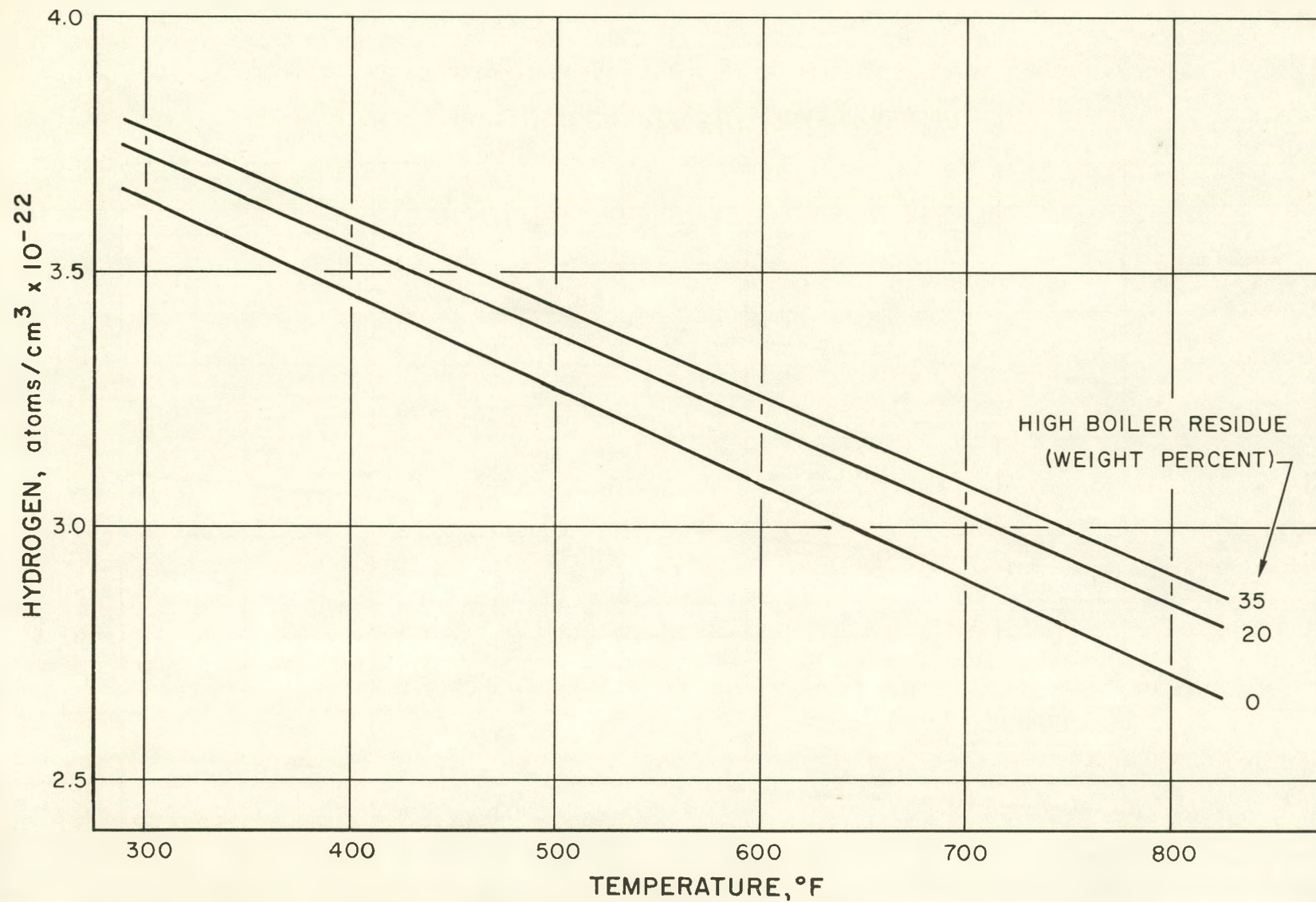


Fig. 7. Hydrogen Density of Irradiated Diphenyl



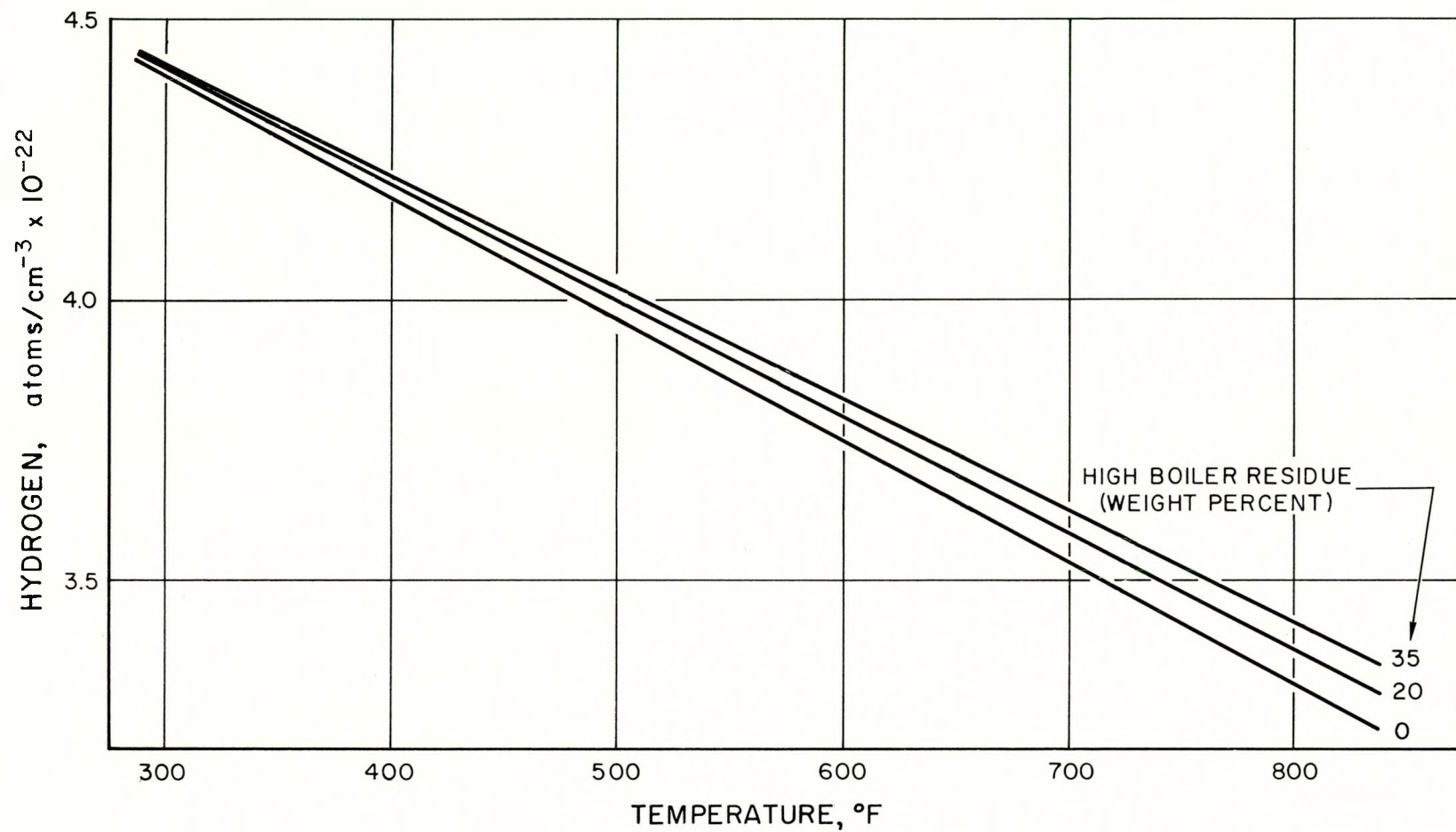


Fig. 8. Hydrogen Density of Irradiated Isopropyl Diphenyl

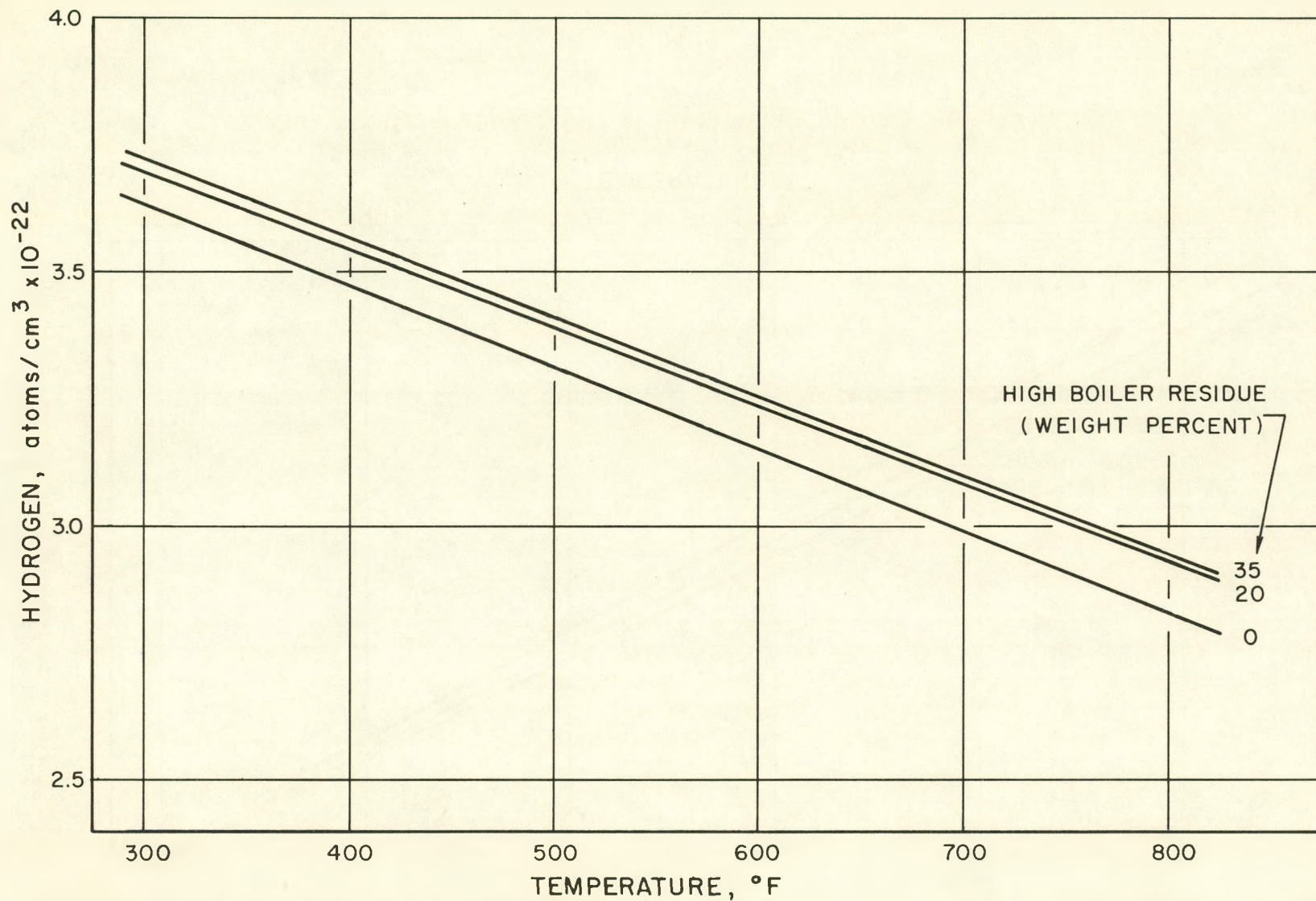


Fig. 9. Hydrogen Density of Irradiated Ortho-, Meta-Terphenyl



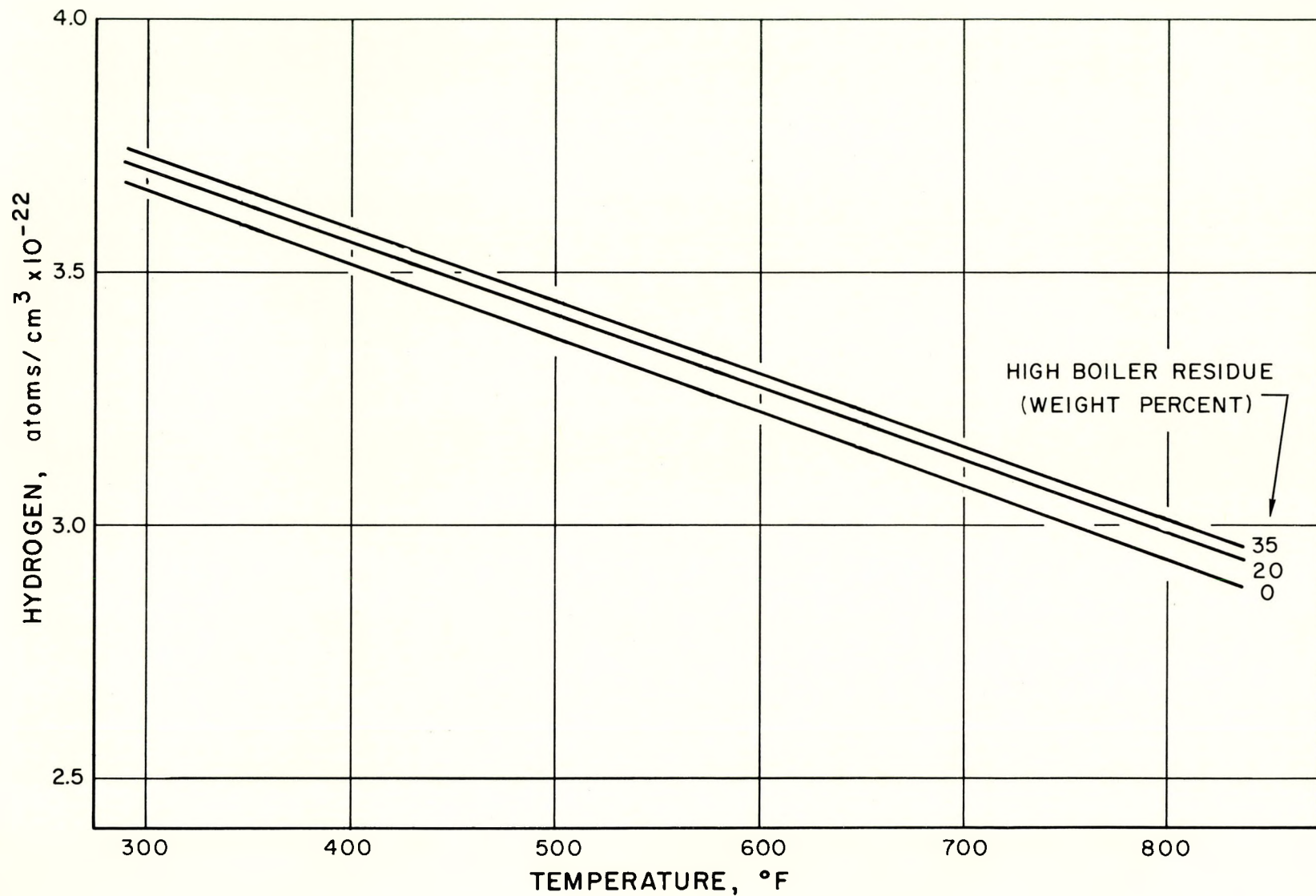


Fig. 10. Hydrogen Density of Irradiated Santowax R



during operation of the NAA-20 organic in-pile loop experiment at the MTR. The starting mixture of ortho-, meta-terphenyl used in the loop test was synthetically compounded to contain 2/3 by weight ortho-terphenyl and 1/3 by weight meta-terphenyl.

The variation of density as a function of temperature with high boiler residue content as a parameter is illustrated in Figs. 11, 12, and 13. The measurements were made with a Lipkin pycnometer, pressurized with helium for the ortho-, meta-terphenyl and Santowax R determinations to prevent boiling. Absolute error in these densities is estimated to be \pm 0.3 percent.

3. Viscosity of Irradiated Ortho-, Meta-Terphenyl

The viscosity of irradiated ortho-, meta-terphenyl has been determined over the temperature range 300 to 850°F. The measurements were made with an Ostwald capillary pipet, pressurized with helium to prevent boiling at the higher temperatures.

The irradiated samples used in these measurements were obtained during operation of the NAA-20 organic in-pile loop at the MTR. The loop starting material was a mixture of ortho-, meta-terphenyl (2/3 by weight ortho-terphenyl). The decomposed samples range in high-boiler-residue content from 0 to 29 weight percent.

The variation of viscosity as a function of temperature with percent high-boiler residue as a parameter is graphically illustrated in Fig. 14. Relative viscosity was determined with an error of approximately 1 percent.

4. Melting Point of Irradiated Diphenyl

The melting point (liquidus) was determined for irradiated diphenyl samples obtained during operation of the long, continuous run (cycles 2082, 2083, and 2084) of the NAA-20 organic in-pile loop. The melting points of the diphenyl samples from the short run (cycle 2078) were also measured.

Within experimental error, the short-run and long-run data fall on the same curve, indicating that no great change is taking place in the nature of the diphenyl decomposition products with increasing length of time of irradiation. These data are shown graphically in Fig. 15.

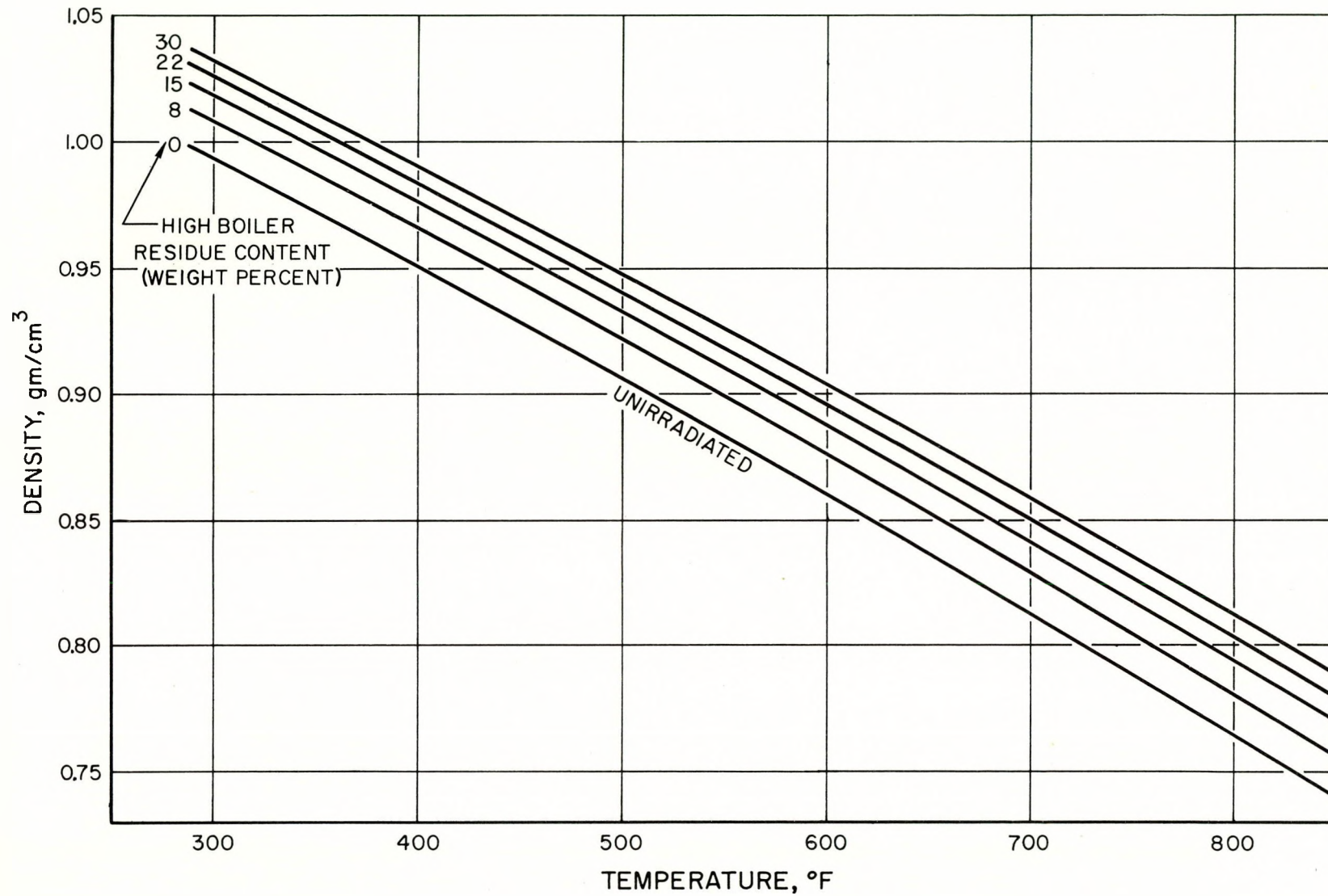


Fig. 11. Density of Irradiated Ortho-, Meta-Terphenyl

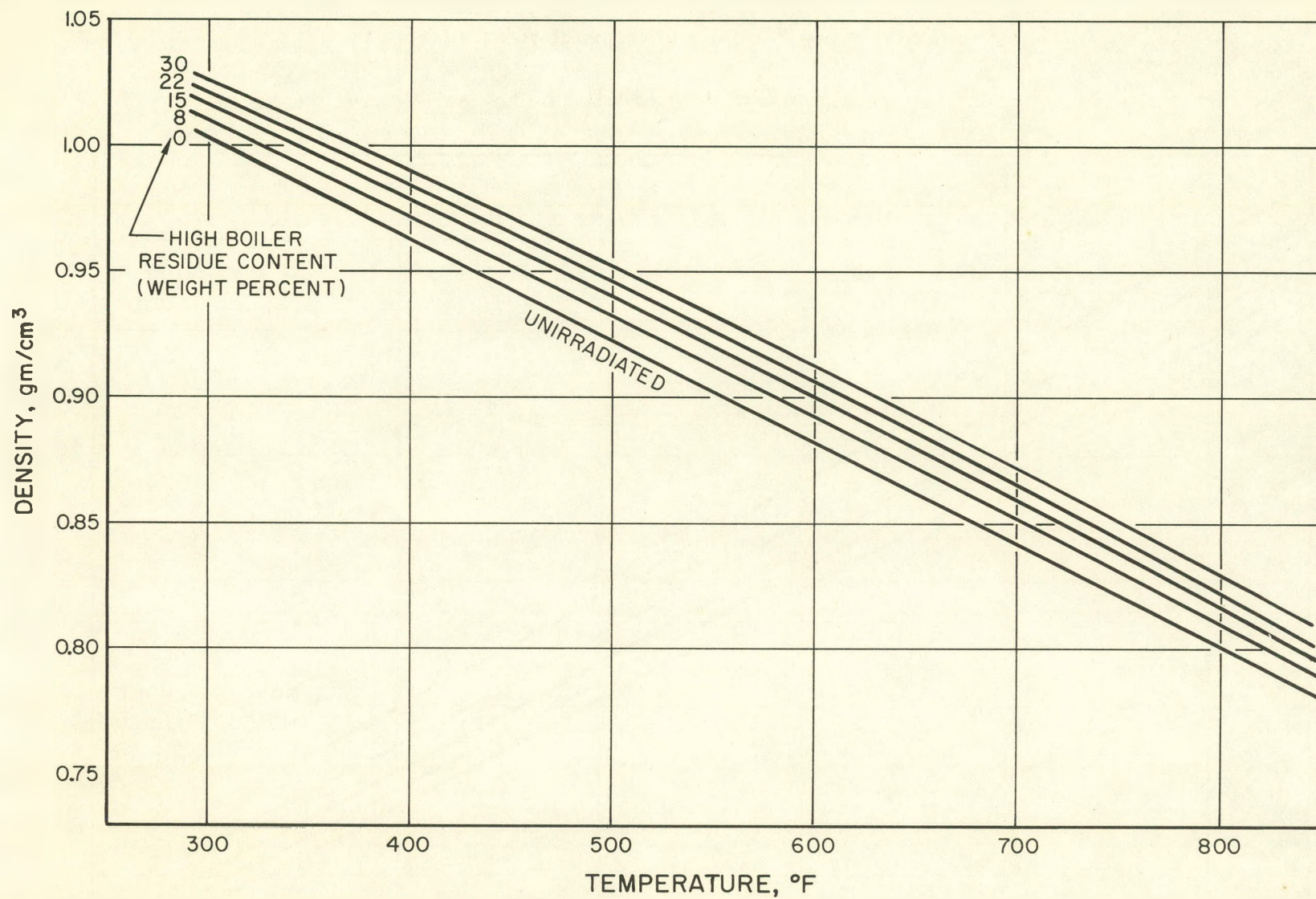


Fig. 12. Density of Irradiated Santowax R



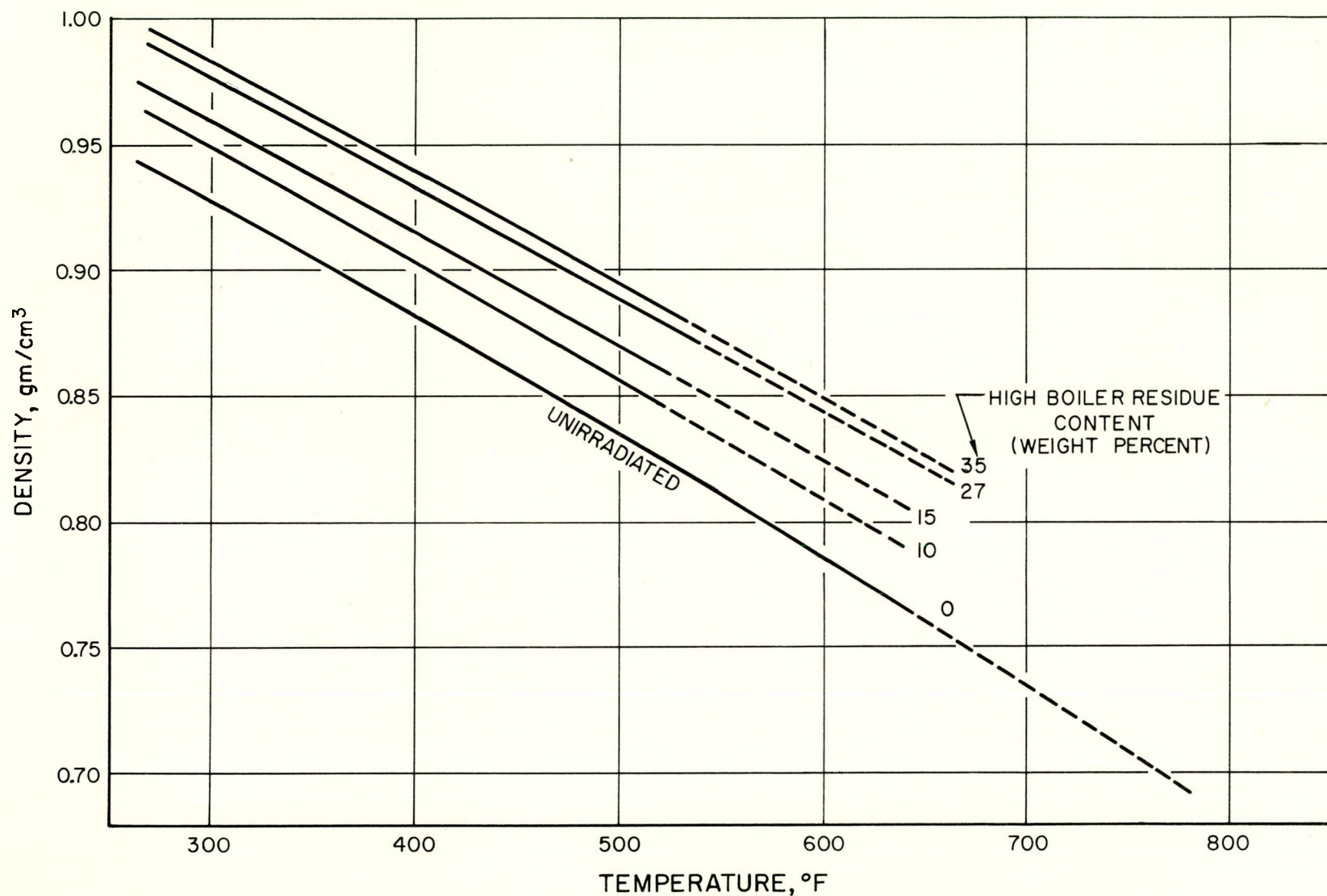


Fig. 13. Density of Irradiated Diphenyl

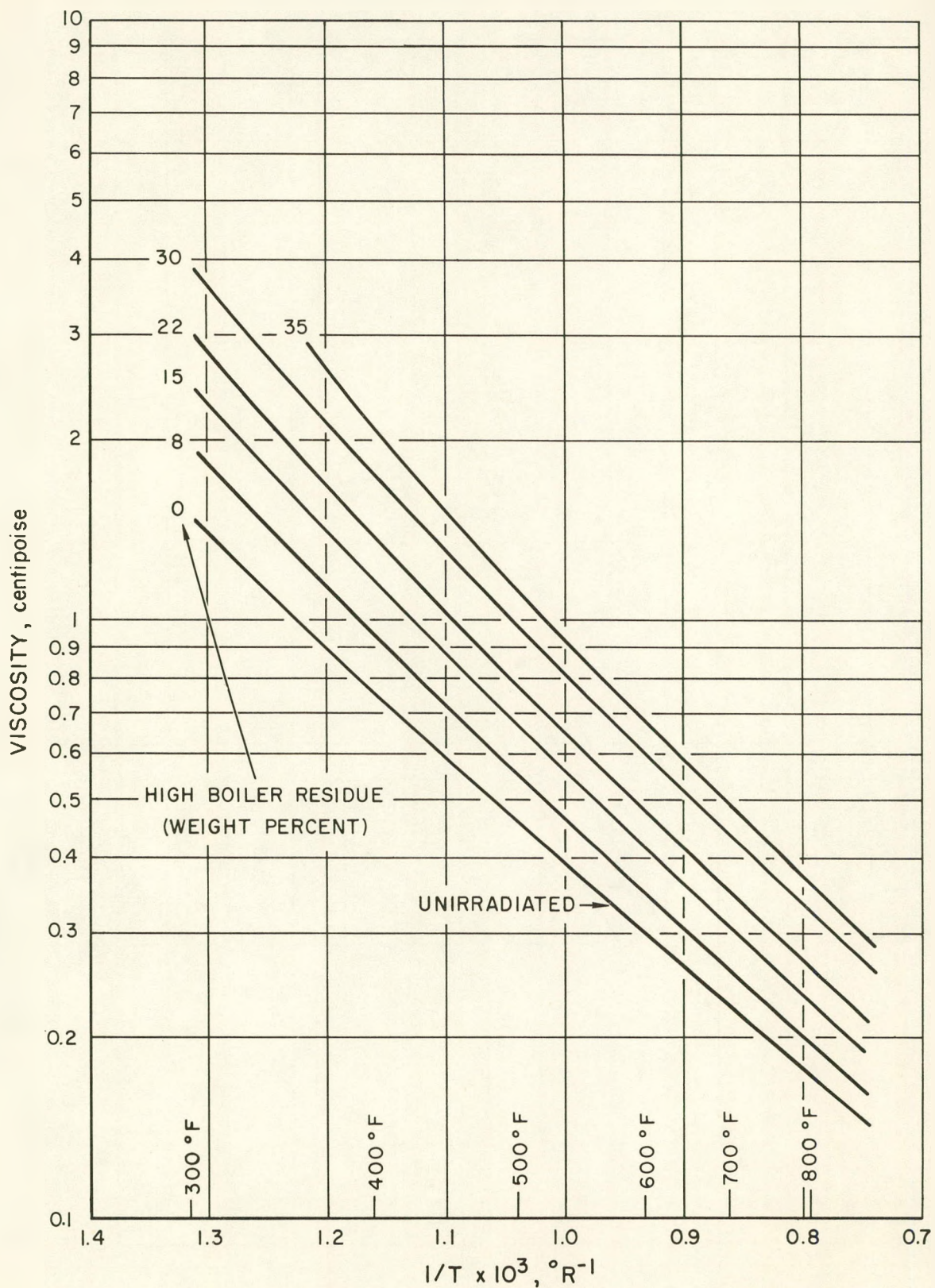


Fig. 14. Viscosity of Irradiated Ortho-, Meta-Terphenyl

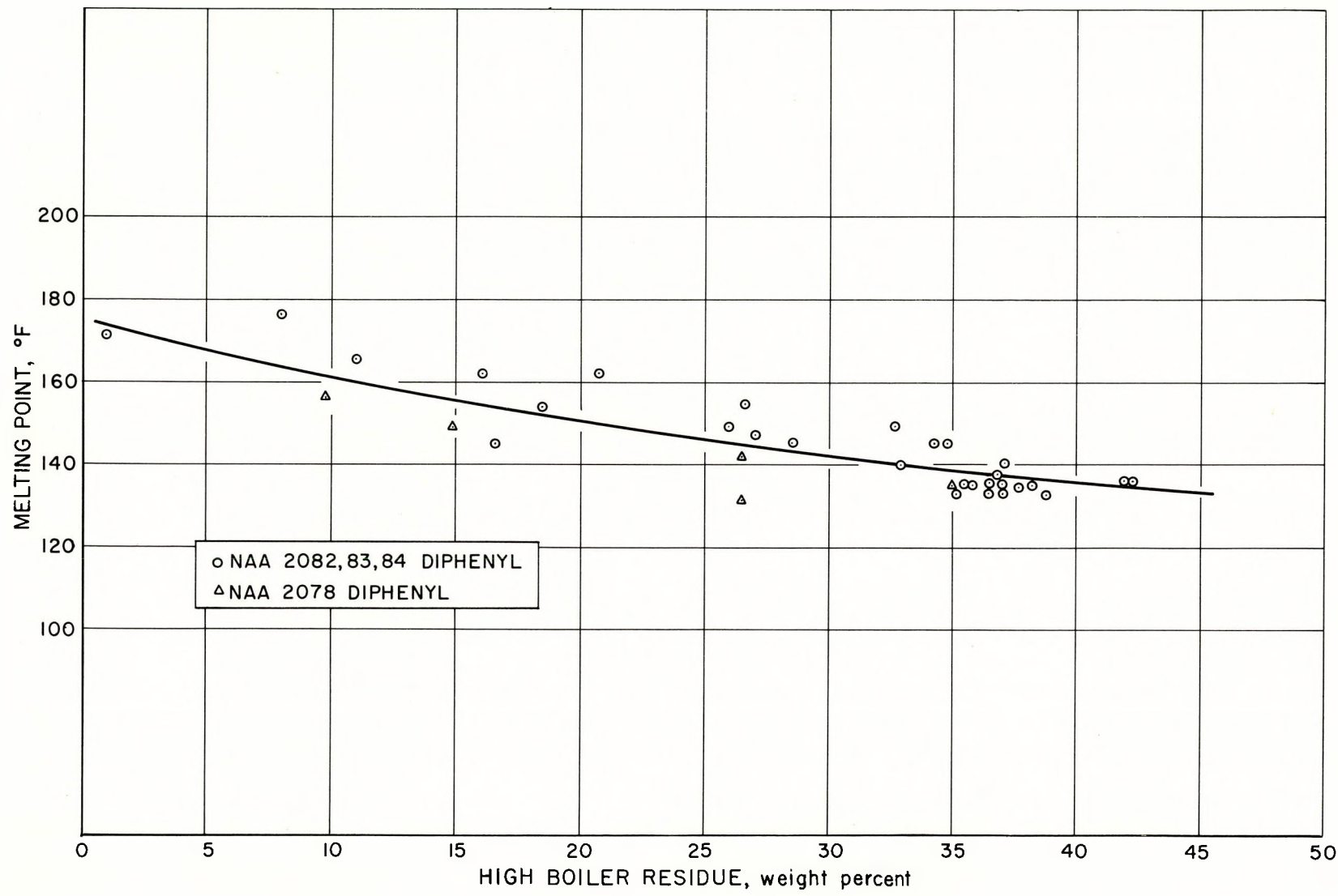


Fig. 15. Melting Point of Irradiated Diphenyl



5. Distillation Curves of Irradiated Coolants

A distillation curve for irradiated coolants is useful in understanding the nature of the decomposition products, and in determining operating conditions for the distillation-purification unit. The distillation curves for several coolants, irradiated during the operation of the NAA-20 organic in-pile loop at the MTR, are shown in Figs. 16, 17, 18, 19, and 20. All of the distillations were carried out at a pressure of 30 mm Hg in a single-plate, all-glass column with continuous take-off.

It is of interest to note that the main fraction of distillate is concentrated in one temperature range for all cases except ortho-, meta-terphenyl, as seen in Fig. 19. This distillation-temperature curve shows a large fraction, about 25 percent of the total sample, located between the initial fraction and the high-boiler-residue range. Figure 20 illustrates the consistent shape of the distillation curve with respect to alternating feed and bleed cycles during operation of the loop experiment. This indicates that only slight variations in the purification unit conditions will be necessary during actual operation of an organic moderated reactor.

6. Ortho-, Meta-Terphenyl OMRE Acceptance Tests

The acceptance tests on samples of ortho-, meta-terphenyl to be used in the OMRE are based on two criteria: (1) allowable impurity content, and (2) melting point. The allowable impurity content was based on an arbitrary maximum permissible radiation level of 500 mr/hr at the 16-inch pipe produced by any individual isotope at a nominal reactor power level of 16 Mw. The maximum permissible concentration in ppm of individual coolant impurities is as follows:

	<u>ppm</u>
Cl	8.9
Mn	0.13
Cu	55

A melting point maximum was set at 235°F.

The acceptance tests on the samples have been completed. The results of melting point and impurity determinations are listed in Table III. In the total number of samples tested, eleven samples were rejected, one for high melting



point and the others for excess impurity content. Sample 27, although it exhibited a melting point above the maximum, was accepted on the basis of low impurity content. In addition, four samples, although they exhibited slightly high impurity contents, were held for possible future use.



TABLE III
OMRE ACCEPTANCE TEST DETERMINATIONS

Sample	Impurities, ppm			M. P., °F (final)	Remarks
	C1	Mn	Cu		
5	2.2	0.07	-	214	†
6	0.63	0.01	-	224	†
7	42.8	0.84	-	-	Reject
8	*	*	-	230	†
9	12.1	0.25	-	221	Hold
10	10.5	0.02	-	208	Hold
11	*	*	-	201	Hold
12	*	*	-	203	†
13	2.0	0.03	-	201	†
14	*	*	-	185	†
15	*	0.06	-	205	†
16	*	*	-	187	†
17	0.5	0.045	-	196	†
18	3.4	0.10	-	192	†
19	3.7	0.17	-	184	Hold
20	41.8	0.06	0.44	192	Reject
21	1.4	0.07	-	181	†
22	3.4	0.05	-	170	†
23	8.4	-	2.8	190	†
24	3.8	0.001	6.3	200	†
25	3.2	-	36.4	207	†
26	2.3	0.004	-	203	†
27	2.0	0.001	-	243	†
28	1.2	0.03	0.12	260	Reject
29	3.4	0.08	-	212	†
30	1.3	0.03	2.3	216	†
31	7.2	-	9.43	205	†
32	2.3	-	0.42	202	†
33	2.1	trace	1.1	180	†

* Not measured quantitatively, but well below acceptable limit.

† Acceptable.



TABLE III (Continued)

OMRE ACCEPTANCE TEST DETERMINATIONS

Sample	Impurities, ppm			M.P., °F (final)	Remarks
	Cl	Mn	Cu		
33	2.1	trace	1.1	180	†
34	1.5	0.021	-	181	†
35	5.7	trace	0.99	187	†
36	0.42	trace	0.09	189	†
37	8.9	trace	0.91	203	†
38	trace	trace	-	199	†
39	2.2	0.064	-	212	†
40	2.4	0.008	1.4	225	†
41	98.6	-	14.3	207	Reject
42	43.7	1.12	-	208	Reject
43	17.6	0.11	-	196	Reject
44	4.2	0.041	-	196	†
45	3.5	0.03	2.1	210	†
46	1.5	-	12.0	192	†
47	0.21	0.19	-	205	†
48	4.1	-	2.0	203	†
49	3.4	0.027	2.2	196	†
50	1.8	0.057	-	196	†
51	3.9	0.19	-	199	Hold
52	4.2	0.035	0.681	201	†
53	4.4	0.061	0.853	185	†
54	20.8	0.11	-	-	Reject
55	4.4	0.20	-	196	Hold
56	29.1	0.49	-	-	Reject
57	28.2	0.55	-	-	Reject
58	36.1	0.12	-	-	Reject
59	5.2	0.032	0.57	183	†
60	-	1.05	1.36	-	Reject
61	2.6	0.056	0.49	163	†

† Acceptable.

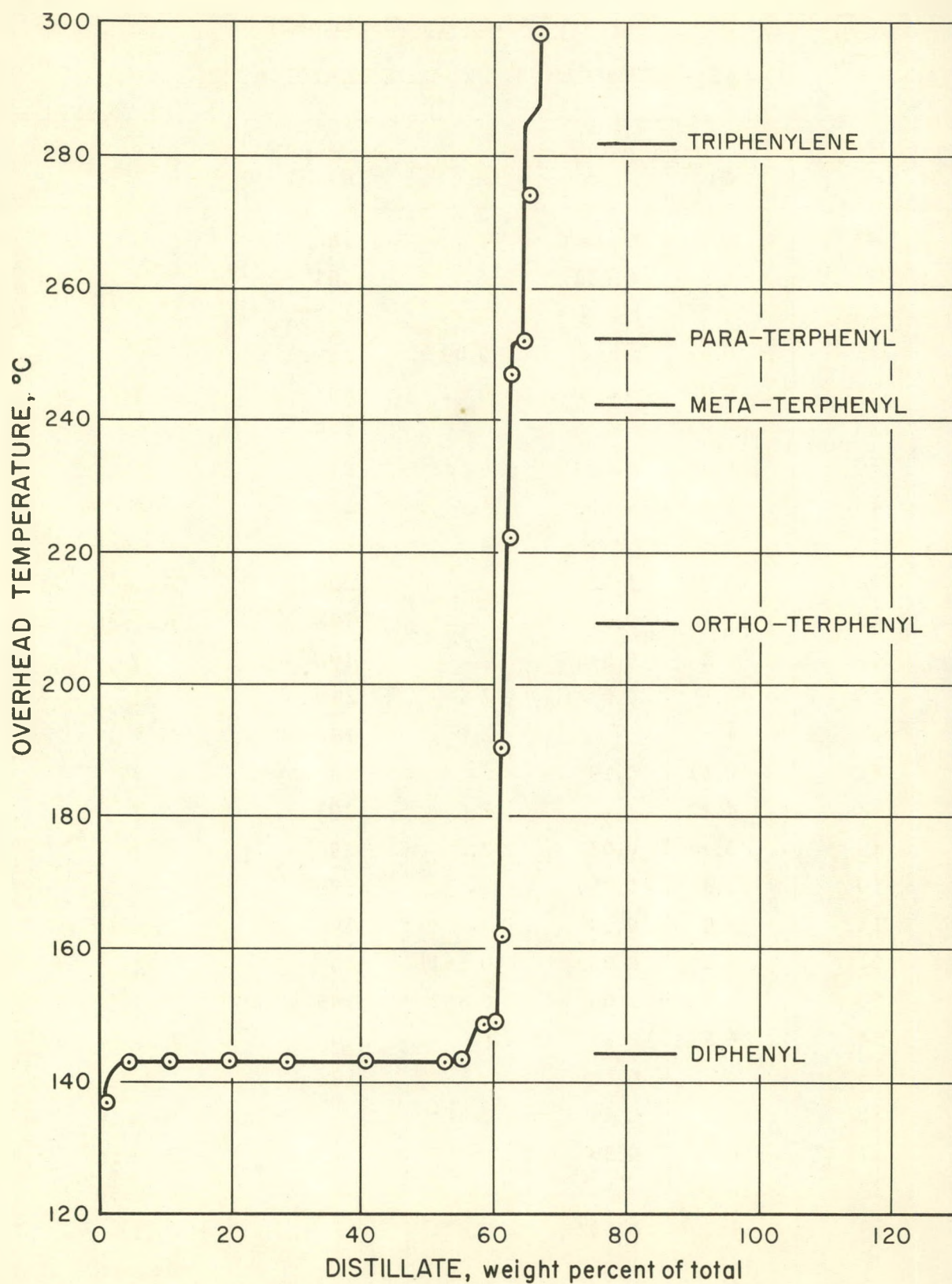


Fig. 16. Distillation Temperature Curve for Irradiated Diphenyl

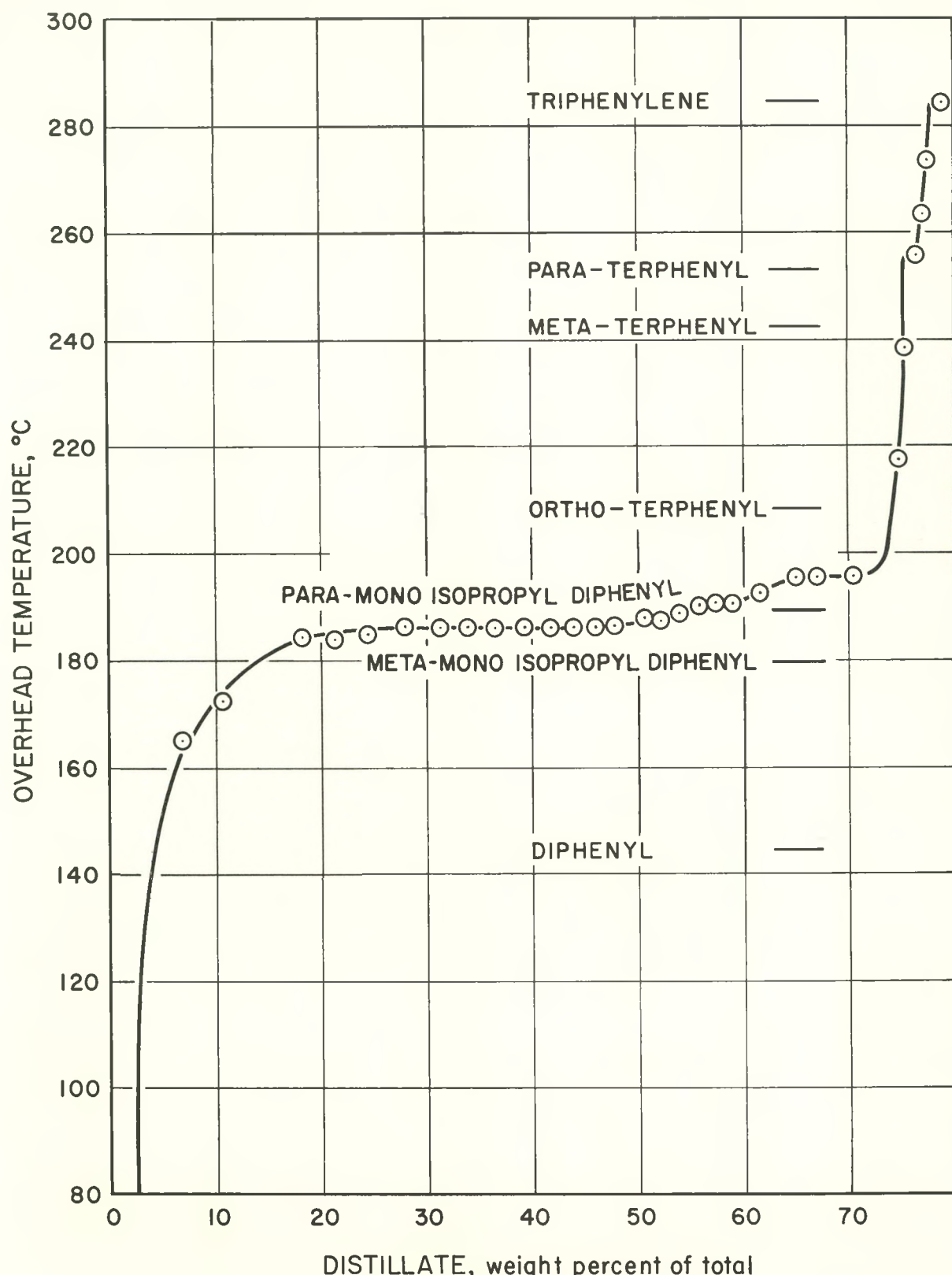


Fig. 17. Distillation Temperature Curve for Irradiated Isopropyl Diphenyl

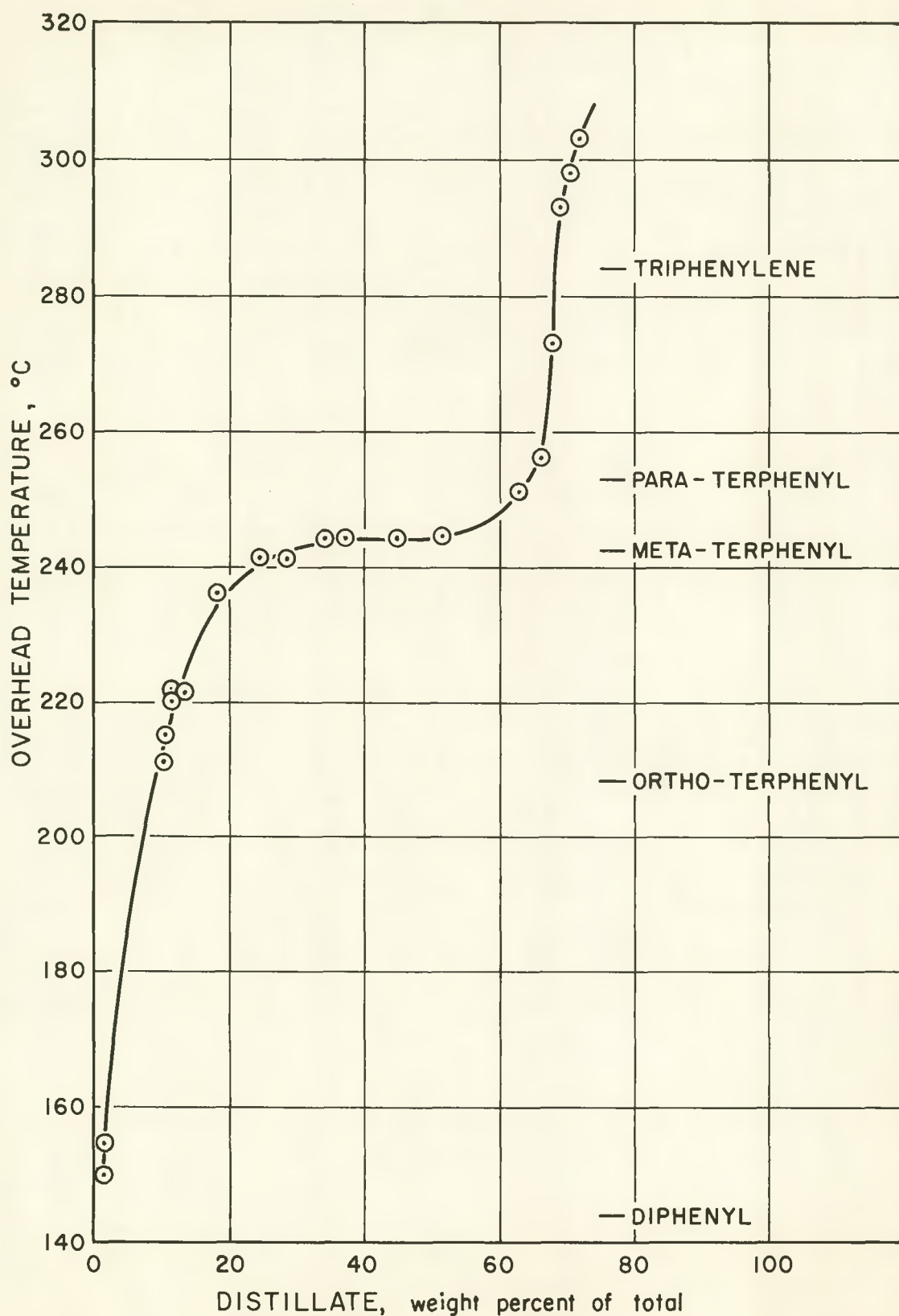


Fig. 18. Distillation Temperature Curve for
Irradiated Santowax R

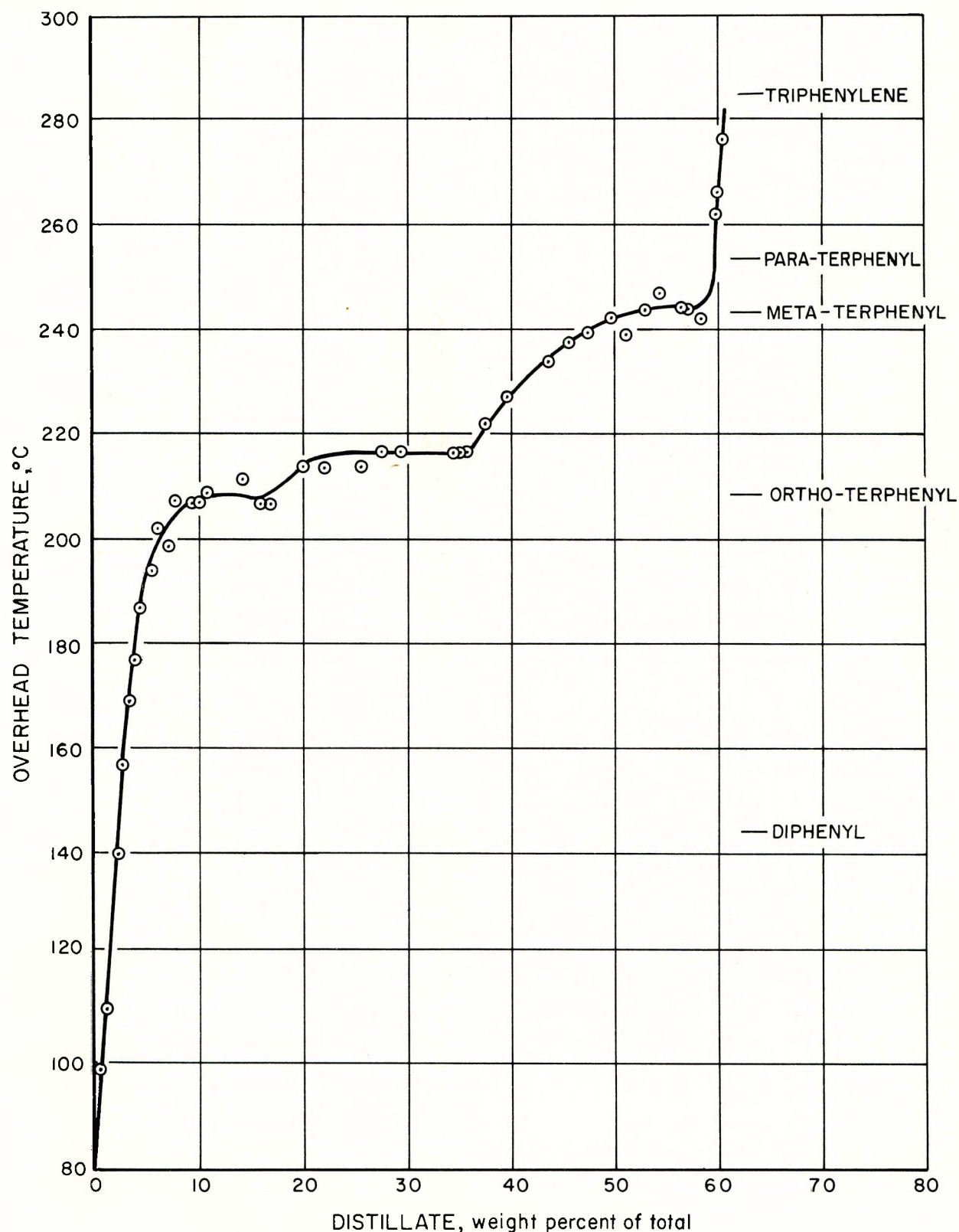


Fig. 19. Distillation Temperature Curve for Irradiated Ortho-, Meta-Terphenyl

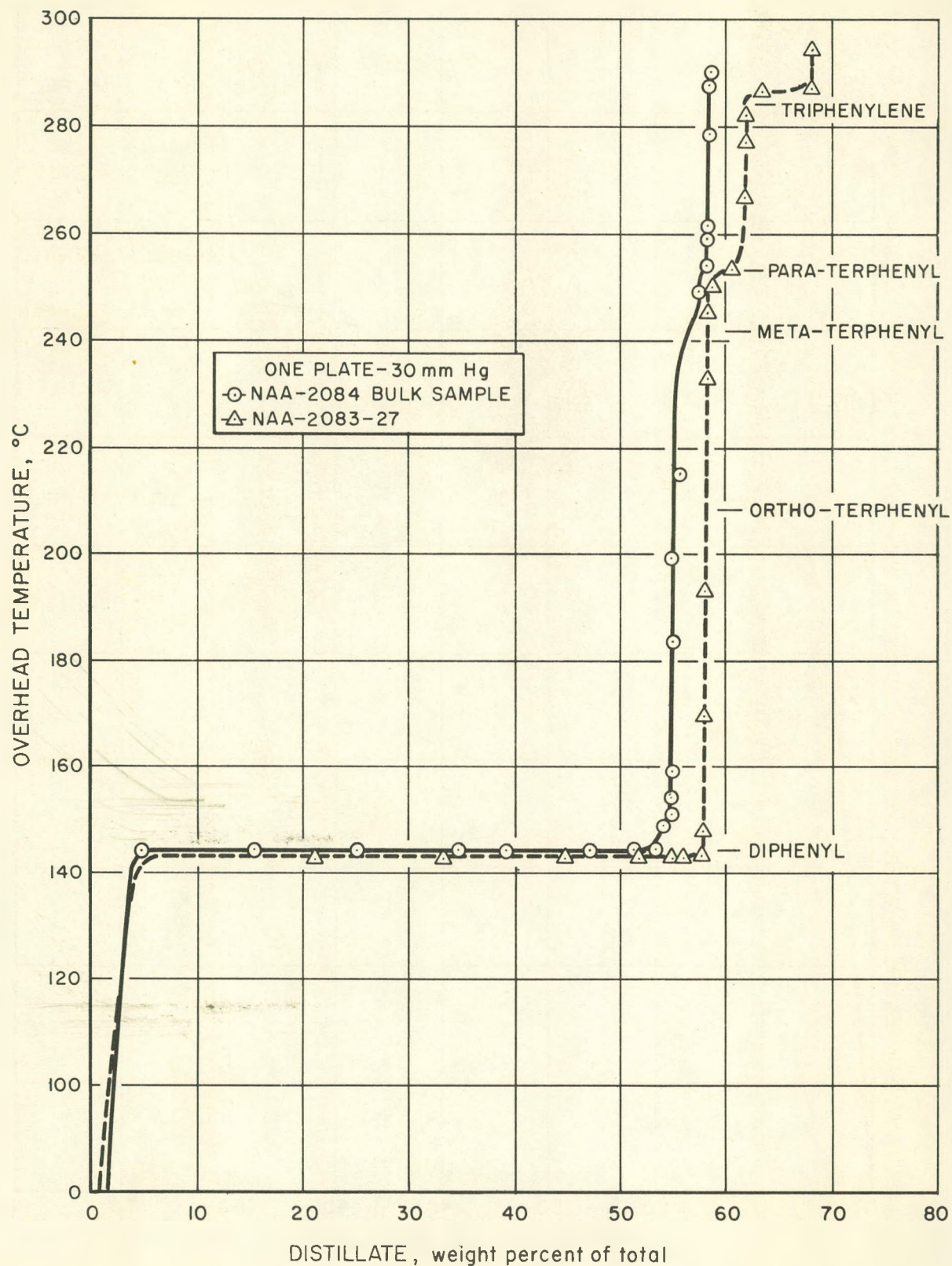


Fig. 20. Distillation Temperature Curve for Irradiated Diphenyl
(Alternate Feed and Bleed Cycles)